A Segment of γ ENaC Mediates Elastase Activation of Na^+ Transport

Adedotun Adebamiro,[1] Yi Cheng,[2] U. Subrahmanyeswara Rao,[3] Henry Danahay,[4] and Robert J. Bridges[2]

[1]Department of Cell Biology and Physiology, University of Pittsburgh, Pittsburgh, PA 15261
[2]Department of Physiology and Biophysics, Rosalind Franklin University of Medicine and Science, North Chicago, IL 60064
[3]School of Pharmacy, Texas Tech. University Health Sciences Center, Amarillo, TX 79106
[4]Novartis Horsham Research Centre, Horsham, West Sussex RH12 5AB, UK

The epithelial Na^+ channel (ENaC) that mediates regulated Na^+ reabsorption by epithelial cells in the kidney and lungs can be activated by endogenous proteases such as channel activating protease 1 and exogenous proteases such as trypsin and neutrophil elastase (NE). The mechanism by which exogenous proteases activate the channel is unknown. To test the hypothesis that residues on ENaC mediate protease-dependent channel activation wild-type and mutant ENaC were stably expressed in the FRT epithelial cell line using a tripromoter human ENaC construct, and protease-induced short-circuit current activation was measured in aprotinin-treated cells. The amiloride-sensitive short circuit current (I_{Na}) was stimulated by aldosterone (1.5-fold) and dexamethasone (8-fold). Dexamethasone-treated cells were used for all subsequent studies. The serum protease inhibitor aprotinin decreased baseline I_{Na} by approximately 50% and I_{Na} could be restored to baseline control values by the exogenous addition of trypsin, NE, and porcine pancreatic elastase (PE) but not by thrombin. All protease experiments were thus performed after exposure to aprotinin. Because NE recognition of substrates occurs with a preference for binding valines at the active site, several valines in the extracellular loops of α and γ ENaC were sequentially substituted with glycines. This scan yielded two valine residues in γ ENaC at positions 182 and 193 that resulted in inhibited responses to NE when simultaneously changed to other amino acids. The mutations resulted in decreased rates of activation and decreased activated steady-state current levels. There was an ∼20-fold difference in activation efficiency of NE against wild-type ENaC compared to a mutant with glycine substitutions at positions 182 and 193. However, the mutants remain susceptible to activation by trypsin and the related elastase, PE. Alanine is the preferred P_1 position residue for PE and substitution of alanine 190 in the γ subunit eliminated I_{Na} activation by PE. Further, substitution with a novel thrombin consensus sequence (LVPRG) beginning at residue 186 in the γ subunit (γ_{Th}) allowed for I_{Na} activation by thrombin, whereas wild-type ENaC was unresponsive. MALDI-TOF mass spectrometric evaluation of proteolytic digests of a 23-mer peptide encompassing the identified residues (T^{176}-S^{198}) showed that hydrolysis occurred between residues V193 and M194 for NE and between A190 and S191 for PE. In vitro translation studies demonstrated thrombin cleaved the γ_{Th} but not the wild-type γ subunit. These results demonstrate that γ subunit valines 182 and 193 are critical for channel activation by NE, alanine 190 is critical for channel activation by PE, and that channel activation can be achieved by inserting a novel thrombin consensus sequence. These results support the conclusion that protease binding and perhaps cleavage of the γ subunit results in ENaC activation.

The Journal of General Physiology

INTRODUCTION

The regulated transepithelial transport of Na^+, critical for maintaining body fluid homeostasis in terrestrial organisms, is attributable to the expression of the heteromeric epithelial Na^+ channel (ENaC) (Garty and Palmer, 1997). ENaC consists of α, β, and γ subunits (Canessa et al., 1994; McDonald et al., 1994). It was previously observed that exogenous aprotinin, a serine protease inhibitor, inhibited Na^+ transport in cortical collecting duct cells from the kidney (Margolius and Chao, 1980; Orce et al., 1980; Vallet et al., 1997; Nakhoul et al., 1998; Vuagniaux et al., 2002) and human bronchial epithelial cells from the lung (Bridges et al., 2001). Epithelial-derived serine proteases such as the channel activating proteases (CAPs, e.g., prostasin) activated ENaC-mediated Na^+ transport when coexpressed in *Xenopus* oocytes (Vallet et al., 1997; Donaldson et al., 2002; Vuagniaux et al., 2002). The ability of some of these proteases, CAP1 and prostasin, to increase Na^+ transport in the coexpression studies was inhibited by aprotinin. In addition to the CAPs, which represent endogenous proteases, ENaC-mediated Na^+ transport can also be activated by exogenous trypsin, chymotrypsin, neutrophil elastase, and cathepsin G (Chraibi et al., 1998; Caldwell et al., 2005; Harris et al., 2007).

The notion that protease activation of Na^+ transport results from cleavage of ENaC arises from the correlation

A. Adebamiro and Y. Cheng contributed equally to this work.
Correspondence to Robert J. Bridges: bob.bridges@rosalindfranklin.edu

The online version of this article contains supplemental material.

Abbreviations used in this paper: CAP, channel activating protease; ENaC, epithelial sodium channel; FRT, fisher rat thyroid; NE, human neutrophil elastase; PE, porcine pancreatic elastase; TFA, trifluoroacetic acid; TH, human alpha thrombin.

between the appearance of cleaved forms of the α and γ subunits and the measured ENaC activity. First, salt restriction or aldosterone infusion (stimuli for increasing Na^+ reabsorption in the kidney) were associated with the appearance of a lower molecular weight γ subunit in the rat cortical collecting duct while control rats had only the heavier γ subunit (Masilamani et al., 1999; Ergonul et al., 2006). Two molecular weight species of the α and γ subunit were found in whole rat kidneys where up-regulation of Na^+ transport in collecting duct cells correlated with an increase of a lower molecular weight fragment of the γ subunit and decrease of the higher molecular weight species suggesting a conversion (Ergonul et al., 2006). Aldosterone up-regulation of prostasin in the cortical collecting duct cells (Narikiyo et al., 2002) may generate the γ subunit cleavage. Further, preventing internalization of ENaC in epithelial cells heterologously expressing ENaC increased the lower molecular weight isoforms of the α and γ subunits at the apical membrane and these changes correlated with decreased sensitivity to exogenous trypsin activation (Knight et al., 2006). Second, mutation of potential furin cleavage consensus sequences found in the α and γ subunits prevented endogenous cleavage of these subunits and reduced Na^+ transport rates (Hughey et al., 2004a; Bruns et al., 2007).

The single channel studies by Caldwell et al. (2004, 2005) provided evidence that exogenously added serine proteases could activate the channel by direct proteolysis. These results suggest that proteases can directly bind to the channel and induce activation by cleavage. Based on the observations that trypsin and human neutrophil elastase could maximally activate silent channels, we tested the hypothesis that proteases directly interact with ENaC, causing activation of Na^+ transport in a model epithelial cell line. Site-directed mutagenesis and analysis of the kinetics of current activation by the related proteases neutrophil elastase and porcine pancreatic elastases as well as thrombin were used to show that specific protease interactions with ENaC occur in a segment of the γ subunit.

MATERIALS AND METHODS

DNA Constructs

Construction of Human α, β, γ ENaC Tripromoter Expression Vector. Standard molecular biology methods were used to construct the ENaC tripromoter expression vector. The human α, β, and γ ENaC subunit cDNAs were isolated from human lung epithelial cells. All three cDNA sequences were identical to the sequence reported by McDonald et al. (1994) (GenBank/EMBL/DDBJaccession nos. L29007, L36592, and L36593). The α cDNA was subcloned into pECFPN1 and a stop codon introduced at the 3′ end of the α subunit to prevent the expression of the CFP. The β and γ subunits were subcloned into the pEGFPN1 vector (CLONTECH Laboratories, Inc.) to obtain pEGFPN1/β and pEGFPN1/γ. Appropriate start and stop codons were inserted to allow for the expression of the β and γ subunits without the C-terminal expression of EGFP. The DNA fragments from pEGFPN1/β and pEGFP/γ vectors comprising the CMV promoters and the subunit cDNA without the GFP sequences were isolated and then subcloned into pECFPN1/α to generate a 13.4-kb tripromoter αβγ hENaC vector (hENaC). The important features of the hENaC vector are that all three ENaC subunits are arranged in tandem and expression of each subunit is under an independent CMV promoter allowing for the separate expression of each subunit without the expression of ECFP or EGFP. Site-directed mutagenesis was performed using Quick Change II XL (Stratagene) for single and double amino acid substitutions. Overlap PCR was performed using Phusion high-fidelity DNA polymerase (Finnzymes) to introduce a human thrombin consensus sequence (LVPRG) by multiple contiguous substitutions in the $\gamma_{186\text{-}190}$ sequence of hENaC. Overlapping fragments were synthesized by PCR with forward and reverse primers 5′-CTCGTGCCAAGAGGCTCAATGTCATGCACATCGAGTCC-3′ and 5′-GCTCCTCAGCAGAATAGCTCATGTTGATTTTCTTCTCC-3′. A second set of forward and reverse primers, 5′-CTGCAGGCCACCAACATCTTTGCACAGGTGCCACAGC-3′ and 5′-GCCTCTTGGCACCAACATCTTTGCACAGGTGCCACAGC-3′, containing Sbf I and BbvC I restriction sites were used in a second round of PCR to yield the blunt end product that was subcloned into the pCR 4Blunt-TOPO vector (Invitrogen), digested with Sbf I/BbvC I, and ligated to the appropriate Sbf I/BbvC I digest fragment of hENaC. V5 C terminal epitope–tagged γ ENaC was generated in pc DNA 3.1 hygromycin (Invitrogen) using a standard two-step overlapping PCR method. The sequences of all mutations were verified by DNA sequencing.

RNA Isolation and RT-PCR Experiments

Total RNA was prepared from parental or hENaC FRT cells, using the ThermoScript RT-PCR System (Invitrogen) according to manufacturer's instructions. cDNA was then subjected to PCR amplification using Finnzymes' Phusion High-Fidelity DNA Polymerase (New England Biolabs, Inc.). Primers were designed for identical sequences in human and rat γ ENaC. Primer sequences were as follows: forward 5′-GGA GAG AAG ATC AAA GCC AAA ATC-3′, reverse 5′-GCA TCT CAA TAC TGT TGG CTG GGC-3′. PCR products were separated on a 0.9% agarose gel and visualized by ethidium bromide staining. Amplified products were confirmed by DNA sequencing.

Cell Culture and Transfection

Fisher rat thyroid (FRT) cells were grown in sodium bicarbonate–buffered Hams's F-12 media (Sigma-Aldrich) modified with 10% FCS (Hyclone), 100 U/ml penicillin, and 100 U/ml streptomycin at 37°C and 5% CO_2 as previously described (Sheppard et al., 1994). The cells were expanded in plastic tissue culture flasks. Confluent monolayers were stably transfected with hENaC or mutant plasmids using Lipofectamine 2000 (Invitrogen) and Opti-MEM media (Invitrogen) as described by the manufacturer's instructions and selected with G418 (500 μg/ml; Invitrogen). The selected cells were fed with media containing 50 μM amiloride. FRT cells were seeded onto permeable tissue culture inserts (Transwell Clear, 0.4 μM pore size, 6 mm diameter; Corning) and fed three times a week with or without supplementation with dexamethasone (30 nM) or aldosterone (30 nM). The cells matured for at least 10 d and amiloride was removed from the feeding media two feeding cycles before short-circuit current measurements.

Short-Circuit Current (I_{SC}) Measurements

Current measurements were performed 10–14 d after seeding. The epithelial cell monolayers were studied by placing the Transwell tissue culture inserts into Costar Ussing chambers with apical and basolateral bathing solution containing (in mM) 120 NaCl, 25 $NaHCO_3$, 3.3 KH_2PO_4, 0.8 K_2HPO_4, 1.2 $MgCl_2$, 1.2 $CaCl_2$, and

10 glucose as previously described (Bridges et al., 2001). The apical and basolateral solutions were continuously circulated with a gas lift. The pH of the solution was 7.4 at 37°C when gassed with a mixture of 95% O_2:5% CO_2. The monolayers were continuously short circuited with a voltage clamp (University of Iowa, Iowa City, IA), and transepithelial resistance was monitored by periodically applying a 4-mV bipolar pulse and calculating resistance from the current change. The amiloride-sensitive I_{SC} (I_{Na}) obtained from the difference in current with and without amiloride (50 μM) in the apical bath was taken as a measure of ENaC-mediated electrogenic Na^+ transport. The amiloride-insensitive current was minimal (<5% of the baseline I_{SC}). Untransfected FRT cells did not show an I_{Na}. The proteases trypsin (Sigma-Aldrich), human neutrophil elastase (NE; EPC), porcine pancreatic elastase (PE; EPC), and human α thrombin (TH; Sigma-Aldrich) were added to the apical bath and mixed by rapid pipetting with a transfer pipette.

Protocol for I_{Na} Activation by Proteases

To observe significant and reproducible protease activation it was necessary to pretreat the cells with the serine protease inhibitor aprotinin. Several epithelia appear to have constitutive activation of Na^+ transport that can be inhibited by aprotinin in a time-dependent manner and the transport rate rapidly reverts to control levels upon addition of exogenous trypsin (Vallet et al., 1997; Bridges et al., 2001; Adebamiro et al., 2005; Myerburg et al., 2006). The slow time dependence of aprotinin inhibition and rapid reversal by excess protease suggests that in the presence of aprotinin, active channels are continually retrieved or degraded while new inactive channels are inserted. This pool of newly inserted channels can then be activated by exogenous proteases. The time course of aprotinin inhibition of current in mammalian airway cells has a half life of ∼45 min (Bridges et al., 2001). To ensure maximal inhibition for all constructs examined in experiments involving pre-protease inhibition, the protease inhibitor, aprotinin (10 μM; Sigma-Aldrich) or a vehicle control (PBS) was added to the apical surface of the monolayers overnight as previously reported (Vallet et al., 1997) in the modified Ham's F-12 media 1 and remained in the apical bath solution during I_{SC} measurements. Overnight treatment reduced the variability in the inhibition of I_{Na} by aprotinin and improved the quantitative analysis of the results.

Data Evaluation and Analysis

The effects of the proteases were assessed in two ways. First, steady-state I_{Na} was assessed before protease addition (baseline I_{Na}), then after the I_{Na} reached a steady-state 20–30 min after addition of NE, PE, or TH (I_{PR}). Trypsin was then added in excess over the aprotinin concentration to obtain I_{Tryp}. To compare the effects of NE, PE, and TH to that of trypsin we used the ratio I_{PR}/I_{Tryp} and the normalized value $\Delta I_{PR}{}^{Norm}$ where $\Delta I_{PR}{}^{Norm} = (I_{PR} - \text{baseline } I_{Na})/(I_{Tryp} - \text{baseline } I_{Na})$. I_{PR} was measured 20–30 min after the addition of protease (NE, PE, or TH) and I_{Tryp} was measured 5 min after the addition of trypsin. Second, following addition of NE, PE, or TH the time course of the $\Delta I_{PR}{}^{Norm}$ in each experiment was analyzed according to two reactions. The first reaction is shown in Eq. 1.

$$C + E \leftarrow \frac{k_{on}}{k_{off}} \rightarrow A \tag{1}$$

The quantity C is the inactive channel at the membrane, E is the added enzyme concentration, and A is the channel activated by proteases. The rate coefficients k_{on} and k_{off} have their usual meanings. The differential equation from Eq. 1 is

$$\frac{d}{dt}(A) = k_{on}E \cdot C_0 - (k_{off} + k_{on}E)A. \tag{2}$$

Under the assumption that the enzyme concentration is constant due to being in excess and there is no autolysis, the differential equation is solved to yield exponential functions in time that can be fitted to the whole time course of current activation (see online supplemental material, available at http://www.jgp.org/cgi/content/full/jgp.200709781/DC1). The time courses for individual experiments were fitted using Matlab (The Mathworks) to Eq. 3.

$$\Delta I_{PR}{}^{Norm}(t) = \Delta I_{PR}{}^{Norm}(\infty)\left(1 - e^{-t/\tau}\right) \tag{3}$$

A linear term was added to Eq. 3 to account for a slow decreasing trend in the current records. The reciprocal of the time constant τ was taken as a measure of the apparent relaxation rate constant k_{obs}. It is shown in the supplemental material that the k_{obs} is given by

$$k_{obs} = k_{off} + k_{on}E. \tag{4}$$

The second reaction is of the form shown in Eq. 5.

$$C + E \leftarrow \frac{k_{on}}{k_{off}} \rightarrow CE \xrightarrow{k_{cat}} A \tag{5}$$

The differential equations from Eq. 5 are

$$\frac{d}{dt}(CE) = k_{on}E \cdot C_0 - (k_{cat} + k_{off} + k_{on}E) \cdot CE - k_{on}E \cdot A \tag{6}$$

$$\frac{d}{dt}(A) = k_{cat} \cdot CE. \tag{7}$$

The k_{off} and k_{on} have their usual meanings and k_{cat} is simply used to express a rate-limiting enzyme concentration-independent step. It is shown in the online supplemental material that the time course of activation can also be approximated by Eq. 3 but here the k_{obs} is given by Eq. 8:

$$k_{obs} = \frac{k_{cat}E}{K_M + E}, \tag{8}$$

where

$$K_M = \frac{k_{off} + k_{cat}}{k_{on}}.$$

Linear and nonlinear regression analysis of the k_{obs} versus enzyme concentration was performed in OriginPro (OriginLab).

Matrix-assisted Laser Desorption Ionization-Time of Flight Analysis (MALDI-TOF)

The sites of cleavage by NE, PE, and TH were searched by MALDI-TOF mass spectrometry on a 23-mer peptide designated peptide T^{176}-S^{198} (Ac-TGRKRKVGGSIHKASNVMHIES-NH_2) and corresponding to the amino acid sequence T176 to S198 of the γ subunit of ENaC. Additional peptides with glycine substitutions at V182, V193, and A190 as well as a peptide substituted with a TH consensus sequence (LVPRG) beginning at residue 186 were evaluated. Enzymatic digestions were performed at 37°C with NE, PE, and TH at final enzyme concentrations of 200 nM and peptide T^{176}-S^{198} at 200 μM in 200 mM Tris acetate, pH 7.4. Following the incubation period, 100 μl of the reaction was quenched by lowering the pH to 3 with addition of 1.0% trifluoroacetic acid (TFA). The reaction without and with the enzymes were subjected to MALDI-TOF measurements. A ZipTip C_{18} solid-phase extraction sorbant (Millipore) was washed with 10 μl of acetonitrile/water

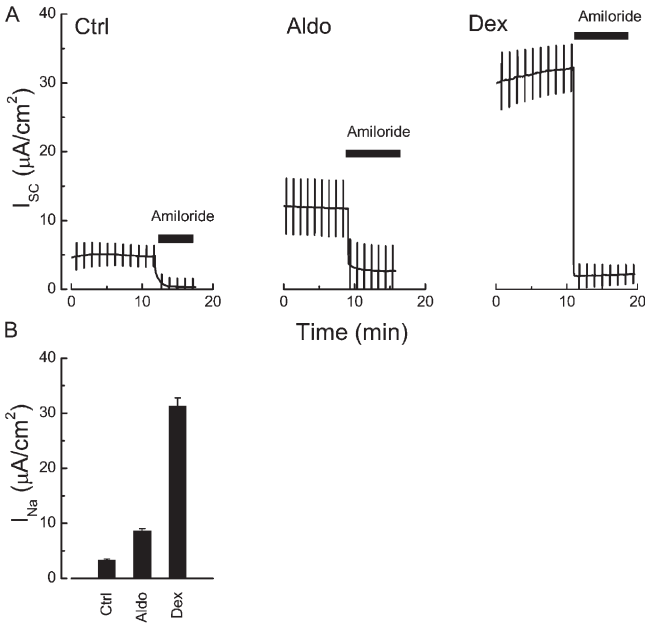

Figure 1. Expression of ENaC and the corticosteroid effect on Na^+ transport in FRT epithelial cells. FRT cells stably transfected with the tripromoter vector containing the α, β, and γ human ENaC subunits were short-circuited in Ussing chambers with symmetrical NaCl, $NaHCO_3$ buffered ringers. (A) Representative current traces of unstimulated (Ctrl), aldosterone (30 nM), and dexamethasone (30 nM) stimulated cells. The vertical deflections are current responses to 4-mV bipolar pulses for monitoring transepithelial resistance. Amiloride (50 μM), was added to the apical side for the indicated period (bars) to determine I_{Na}, the amiloride-sensitive component of the I_{SC}. (B) Summary of the amiloride-sensitive I_{Na} (mean ± SEM; n = 7–11).

(1:1, vol/vol) and then equilibrated with aqueous 0.1% TFA. Peptide samples acidified with 5% aqueous TFA to enhance peptide retention on the stationary phase of the C_{18} sorbant were loaded onto the tip and eluted with 0.1% TFA in acetonitrile/water (1:1, vol/vol). The matrix solution was prepared by dissolving 10 mg of cyano-4-hydroxycinnamic acid in 1 ml of acetonitrile/water (1:1, vol/vol) containing 0.1% TFA. 0.5 μl of the matrix solution was mixed with 0.5 μl of peptide solution. About 0.5 μl of the mixture was deposited onto the MALDI stage and air dried. Positive ion MALDI-TOF Mass spectra were acquired on an Applied Biosystems Voayger DE-Star mass spectrometer operated in reflector mode. Following time-delayed extraction, the ions were accelerated to 20 kV for TOF analysis. A total of 100 laser shots were acquired and signal averaged per spectrum.

In Vitro Translation and Western Blots

cDNAs were transcribed and translated in vitro in the presence of canine pancreatic microsomal membranes using the TnT-coupled reticulocyte lysate systems (Promega). Total DNA templates (0.5 μg) containing 0.25μg αβ and 0.25μg γ-V5 or 0.25 μg of γ_{Th}-V5 ENaC subunits were added to an aliquot of the TnT T7 Quick Master mix containing 2 μl microsomal membranes and incubated at 30°C for 60 min. The translation products were collected by centrifuging for 15 min at ~10,000 *g*. and subjected to lysis in 1% Triton X-100 buffer (1% Triton X-100, 500 mM NaCl, 5 mM EDTA, 50 mM Tris-HCl, pH 7.5) at 4°C . The lysates were incubated for 5 min at 37°C in the presence or absence of 200 nM human α thrombin (Sigma-Aldrich). All samples in 1× SDS-PAGE sample buffer containing 100 mM DTT were heated for 10 min at 70°C before loading. Proteins were separated on NuPAGE 4–12% Bis-Tris Gel (Invitrogen) and were transferred to Immobilon-P membrane (Millipore). Proteins were detected by Western blot with mouse monoclonal anti-V5 antibody (Invitrogen) targeting a V5 epitope on the C terminus of the γ ENaC subunit. The signal was developed with the Supersignal west femto maximum sensitivity substrate (Pierce Chemical Co.) and detected with X-Omat Blue XB-1 imaging film (Kodak).

Statistics

Effects of the proteases on steady-state I_{Na} for the wild-type hENaC were determined using paired t tests of (1) I_{Na} at baseline versus I_{PR} or I_{Tryp} and (2) I_{PR} versus I_{Tryp}. Comparison of the ratio of ΔI_{PR}^{Norm} and τ across multiple mutants was performed with one-way ANOVA followed by individual comparisons versus wild-type ENaC using the Bonferroni corrected t test in Origin . $P < 0.05$ was considered significant.

Online Supplemental Material

The online supplemental material (available at http://www.jgp.org/cgi/content/full/jgp.200709781/DC1) provides the derivations of Eqs. 3 and 8 where the solutions todifferential Eqs. 2, 6, and 7 are given.

RESULTS

Expression of ENaC-mediated Na^+ Transport in FRT Cells and Regulation by Corticosteroids and Protease

FRT epithelial cells stably transfected with the α, β, and γ human ENaC subunits in a single tripromoter vector (hENaC) had an I_{SC} that was blocked by addition of amiloride (50 μM) to the apical side (Fig. 1, A and B). The magnitude of the amiloride-sensitive I_{SC} (I_{Na}) averaged 3.4 ± 0.12 μA/cm² (n = 11) and is similar to what has been typically observed by transiently transfecting FRT cells simultaneously with the three ENaC subunits in separate plasmids (Snyder, 2000). Feeding the cells in media supplemented with either aldosterone (30 nM) or dexamethasone (30 nM) for 72 h or more before short circuiting significantly increased I_{Na} with no increase in the amiloride-insensitive I_{SC}. Aldosterone induced a 1.5-fold (n = 7) increase in I_{Na} while dexamethasone induced an eightfold (n = 11) increase in I_{Na} (Fig. 1 B). The half maximal inhibitory concentration (K_i) for amiloride was 570 ± 86 nM with a maximal inhibition of 96 ± 1.2%. To determine whether proteases regulate Na^+ transport in FRT cells stably expressing hENaC, the effect of exogenously added trypsin and protease inhibitor were examined. The cells were first preincubated either with the protease inhibitor aprotinin (10 μM) or a vehicle control (PBS) on the apical side for 16–24 h. The cells that were preincubated with aprotinin had decreased I_{Na} compared with cells preincubated with PBS. During short circuiting, addition of trypsin (15 μM) to the apical bath, in a 5 μM excess over the aprotinin concentration, caused no statistically significant increase in the I_{Na} of PBS-preincubated cells (3.9 ± 0.87 to 4.5 ± 1.03 μA/cm²; n = 11) but significantly increased I_{Na} in aprotinin-pretreated cells.

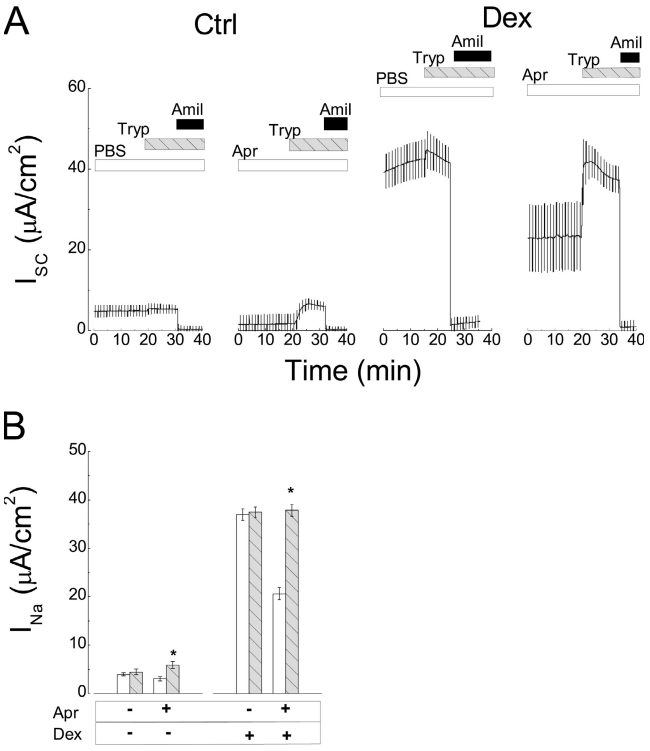

Figure 2. Na^+ transport regulation by aprotinin and trypsin in FRT epithelial cells. (A) Representative I_{SC} traces in FRT cells expressing ENaC, preincubated with and kept in vehicle (PBS) control or aprotinin (APR; 10 μM) during short-circuiting as indicated by the bars. Also shown are traces from cells prestimulated with dexamethasone (30 nM). Trypsin (15 μM) and amiloride (50 μM) were added to the apical side as indicated (horizontal bars). (B) I_{Na} (mean ± SEM, n = 11–18) before (open bars) and after (solid bars) addition of trypsin in PBS-preincubated cells and aprotinin-preincubated cells without or with dexamethasone stimulation as indicated. *, $P < 0.05$ by paired Student's t test comparison of I_{Na} at baseline and after addition of trypsin (I_{Tryp}).

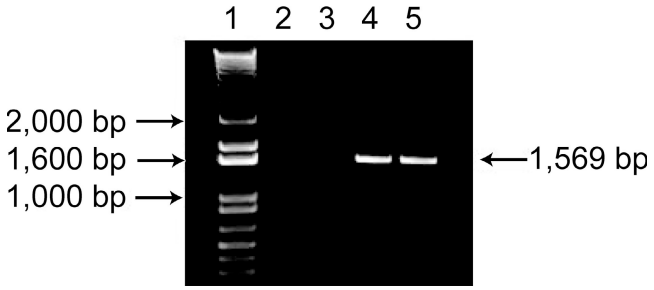

Figure 3. RT-PCR analysis of γ ENaC expression in parental and hENaC-FRT cells. RNA was isolated from parental or hENaC-FRT cells. PCR products were obtained with specific primers spanning identical nucleotide sequences in rat and human γENaC. PCR products were separated on a 0.9% agarose gel and visualized by ethidium bromide staining. Lane 1, standard DNA marker with 1-kb Plus DNA ladder; lanes 2 and 3, RT-PCR of RNA derived from parental cells; lanes 4 and 5, RT-PCR of RNA derived from hENaC FRT cells. Cells for lanes 3 and 5 were treated with 30 nM dexamethasone. The expected PCR product of 1569 bp was detected only in hENaC-FRT cells.

The baseline I_{Na} in the aprotinin-pretreated cells was 3.1 ± 0.68 and the maximal I_{Na} after addition of trypsin (I_{Tryp}) was 5.9 ± 0.68 μA/cm² (n = 12). No differences were found in the trypsin-activated current between PBS- and aprotinin-treated cells. Consequently, aprotinin unmasks a portion of I_{Na} that can be regulated by extracellular protease activity similar to the previously reported effects of aprotinin and trypsin. The absolute values of the aprotinin and trypsin effects on I_{Na} were greatly enhanced in dexamethasone-treated cells but displayed the same qualitative pattern (Fig. 2, A and B). As already noted, dexamethasone treatment greatly increased the I_{Na} (37.0 ± 1.19 μA/cm², n = 18). Trypsin addition had no effect on I_{Na} (37.1 ± 1.14 μA/cm², n = 18) in PBS-pretreated dexamethasone-stimulated cells. Pretreatment with aprotinin caused a 50% decrease in the baseline I_{Na} (21.3 ± 0.85 μA/cm², n = 18) and in aprotinin-inhibited cells trypsin doubled the I_{Na} (40.8 ± 2.09 μA/cm², n = 18) to the value observed in PBS-pretreated cells (Fig. 2, A and B). An excess of trypsin above the aprotinin concentration was required to stimulate I_{Na}. In addition, the stimulatory effects of trypsin on I_{Na} in aprotinin-treated cells was blocked by soy bean trypsin inhibitor (ΔI_{Na} with SBTI 0.7 ± 1.22 μA/cm², n = 6). Because the dexamethasone-stimulated hENaC-expressing FRT cells gave a more robust and reproducible I_{Na} and the protease regulatory pattern persists in dexamethasone-treated cells, dexamethasone-treated cells were used in the remainder of the study. Dexamethasone treatment of untransfected FRT cells did not produce amiloride- or trypsin- sensitive I_{SC}. In untransfected parental cells treated with PBS, the I_{SC} before trypsin, after trypsin, and after amiloride addition were 0.1 ± 0.06, 0.2 ± 0.06, and 0.2 ± 0.07 μA/cm² (n = 12), respectively. For cells treated with aprotinin, the I_{SC} were 0.7 ± 0.3, 0.5 ± 0.16, and 0.5 ± 0.16 μA/cm² (n = 12) before trypsin, after trypsin, and after amiloride, respectively. Furthermore, in cells treated with 30 nM dexamethasone that were stably transfected with the α and β hENaC subunits but without the γhENaC subunit there was no I_{Na} before trypsin (0.2 ± 0.12) μA/cm², after trypsin (0.3 ± 0.08 μA/cm²), and amiloride (0.4 ± 0.09 μA/cm², n = 6). RT-PCR analysis of RNA derived from parental FRT cells without or with dexamethasone treatment did not detect any PCR product for rat γENaC but the expected γ hENaC product was detected with RNA derived from the hENaC-transfected FRT cells (Fig. 3). Thus dexamethasone-stimulated expression of endogenous rat γENaC and complementation with α and β hENaC subunits cannot explain the I_{Na} observed in our studies. The importance of this assertion will become apparent in subsequent results.

In addition to modulating sodium transport, aprotinin and trypsin also altered the transepithelial resistance (R_T). Aprotinin treatment caused a 50% decrease in R_T

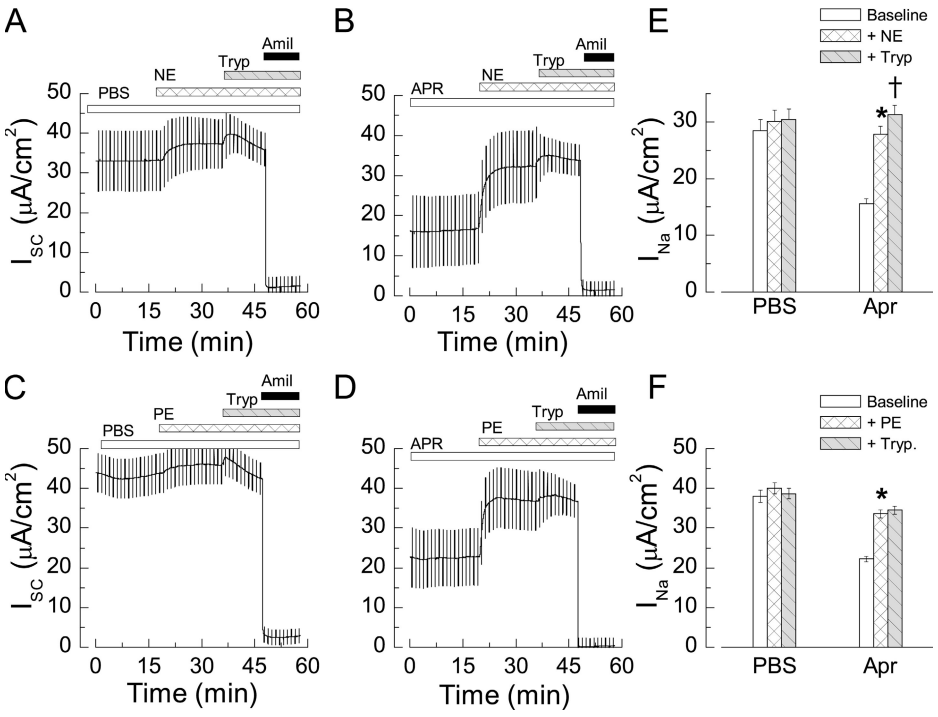

Figure 4. Elastase-mediated activation of ENaC in FRT cells. (A–D) Representative I_{SC} in FRT cells expressing ENaC that were either pretreated with PBS (A and C) or with 10 μM aprotinin (B and D). (A and B) NE (300 nM) or (C and D) PE (300 nM) was added to the apical bath of short-circuited cells. Trypsin (15 μM) and amiloride (50 μM) were subsequently added to the apical baths in all experiments as indicated (horizontal bars). (E) I_{Na} (mean ± SEM, n = 16–24) before (open bars), after 300 nM of NE or (F) PE (stripped bars), and after 15 μM trypsin (shaded bars). *, $P < 0.05$ in paired Student's t tests of baseline I_{Na} and after NE or PE addition. †, $P < 0.05$ in paired student's t tests of I_{Na} after NE/PE and after trypsin.

compared with PBS-treated hENaC-FRT cells (aprotinin 502 ± 47 Ω cm² vs. PBS 769 ± 45 Ω cm², n = 6) and this effect was reversed by trypsin (aprotinin plus trypsin 1555 ± 125 Ω cm² vs. PBS plus trypsin 1215 ± 101 Ω cm², n = 6). Amiloride further increased R_T in both aprotinin- and PBS trypsin–treated cells to 2614 ± 164 Ω cm² and 3592 ± 289 Ω cm² (n = 6), respectively. Amiloride, when added before trypsin, did not prevent the increase in R_T caused by trypsin in the aprotinin-treated cells (Δ R_T aprotinin plus trypsin 1053 Ω cm² vs. Δ R_T aprotinin plus amiloride plus trypsin 1113 Ω cm², n = 3). The effects of aprotinin and trypsin on R_T were also observed in parental untransfected FRT cells (unpublished data) and these effects have been reported by others in different epithelia (Lynch et al., 1995; Liu et al., 2002). It has been suggested these effects are due to changes in the resistance of the tight junction (Meyer et al., 1988; Kemmner and Zaar, 1991). Serosal to mucosal fluxes of the extracellular maker mannitol revealed aprotinin treatment increased the flux by 60% when compared with PBS-treated hENaC FRT cells (aprotinin 1.3 ± 0.04 nMol/h/cm² vs. PBS 0.8 ± 0.05 nMol/h/cm², n = 6) and this effect was reversed by trypsin (aprotinin plus trypsin 0.4 ± 0.07 nMol/h/cm² vs. PBS plus trypsin 0.5 ± 0.05 nMol/h/cm², n = 6). Because we studied sodium transport under short-circuited conditions and in symmetric solutions these changes in the paracellular pathway resistance are not expected to influence our measurements of I_{Na}. Furthermore as shown below NE, PE, and thrombin do not alter R_T but do increase I_{Na} in aprotinin-treated hENaC-FRT cells.

Submicromolar Neutrophil and Porcine Elastase Activate ENaC in FRT Cells

It was previously shown that, like trypsin, NE can activate ENaC-mediated Na^+ current (Caldwell et al., 2005; Harris et al., 2007). We examined the effect of NE and PE, a similar elastase (Baugh and Travis, 1976; Travis et al., 1979), on the I_{SC} in FRT cells expressing hENaC. Elastase is not inhibited by aprotinin (Baugh and Travis, 1976; Ohlsson and Olsson, 1976), therefore an excess over the aprotinin concentration was not required to stimulate I_{Na}. Addition of NE (300 nM) or PE (300 nM) to the apical side of FRT cells expressing hENaC did not alter the I_{Na} in cells pretreated with PBS (Fig. 4 and Table I). Subsequent addition of trypsin did not further increase the I_{Na} in PBS pretreated cells. Similar to the effects of trypsin NE and PE clearly increased the I_{Na} in cells that were pretreated with 10 μM aprotinin as shown in Fig. 4 (B and D). The rise in the I_{Na} following elastase addition occurred over a 5-min period and increased to a plateau value equal to the baseline I_{Na} of uninhibited cells that were preincubated with PBS. Addition of trypsin subsequent to NE or PE produced small further increases in the I_{Na} in aprotinin-treated cells ($P < 0.01$). The irreversible NE inhibitor MeOSuc-Ala-Ala-Pro-Ala-CMK at 4 μM nearly completely prevented the stimulation of I_{Na} by NE (300 nM) (ΔI_{Na} without inhibitor 24.1 ± 4.21 μA/cm², n = 6; ΔI_{Na} with inhibitor 2.7 ± 0.60 μA/cm², n = 6) and confirm the results of Harris et al. (2007) using a novel NE inhibitor in *Xenopus* oocyte studies. Thus, NE or PE increased I_{Na} in aprotinin-inhibited cells to the values observed in control PBS-treated cells and only a small additional further stimulation was seen with trypsin

TABLE I

Protease Effect on Amiloride Sensitive Short-Circuit Current (I_{Na}) in Cells Expressing Wild Type or Selected Glycine Scan Substitutions

Construct	PBS				Aprotinin			
	Baseline I_{Na}	I_{PR}	I_{Tryp}	*n*	Baseline I_{Na}	I_{PR}	I_{Tryp}	*n*
		$\mu A/cm^2$				$\mu A/cm^2$		
WT	28.5 ± 1.96	30.1 ± 2.01	30.4 ± 1.84	26	15.6 ± 0.86	27.8 ± 1.40[a]	31.3 ± 1.60[c]	36
α_{V171G}	23.7 ± 1.11	22.4 ± 1.67	23.6 ± 2.37	6	11.6 ± 0.37	26.0 ± 1.59[a]	24.9 ± 1.46[b]	6
α_{V193G}	18.1 ± 1.25	18.2 ± 1.48	20.8 ± 0.71	6	10.2 ± 0.61	25.6 ± 1.01[a]	25.3 ± 1.71	6
α_{V206G}	27.5 ± 0.61	32.5 ± 2.16	31.9 ± 2.17	3	18.6 ± 0.95	34.2 ± 0.84[a]	39.5 ± 1.52[b]	3
γ_{V110G}	35.7 ± 2.22	32.8 ± 2.13	30.5 ± 2.09[b]	3	22.9 ± 1.36	31.6 ± 2.02[a]	31.7 ± 2.74	3
$\gamma_{V110;V146G}$	38.6 ± 1.04	40.0 ± 1.78	38.8 ± 1.24	6	21.7 ± 1.75	35.4 ± 3.47[a]	40.4 ± 1.54	6
γ_{V182G}	30.7 ± 1.80	30.7 ± 1.64	29.5 ± 1.28[b]	17	15.8 ± 0.84	28.6 ± 1.44[a]	32.5 ± 1.09[c]	24
γ_{V193G}	37.5 ± 4.02	37.0 ± 4.14	36.7 ± 3.12	6	16.6 ± 0.59	32.0 ± 2.18[a]	37.5 ± 2.12[c]	13
$\gamma_{V182G;193G}$	32.7 ± 1.46	33.0 ± 1.50	34.8 ± 1.15[b]	29	18.3 ± 0.67	25.9 ± 1.07[a]	38.9 ± 1.12[c]	39

The concentration of NE and trypsin added sequentially to the apical bath were 300 nM and 15 μM, respectively. The data is reported as mean ± SEM (*n*, number of observations).

[a]$P < 0.05$, paired Student's *t* tests of baseline I_{Na} versus I_{PR}.

[b]$P < 0.05$, paired student's *t*-tests of I_{PR} and I_{Tryp}.

[c]$P < 0.01$, paired student's *t*-tests of I_{PR} and I_{Tryp}.

addition in the case of NE-stimulated cells (Fig. 4, E and F, and Table I).

Identification of Elastase-specific Sites I: Human Neutrophil Elastase

To determine whether specific sites on ENaC mediate the NE-dependent activation of I_{Na}, we performed site-directed mutagenesis of possible NE binding or hydrolytic sites in the extracellular loops of α and γ ENaC subunits. NE hydrolyzes polypeptides with a strong preference for cleavage of V-X bonds where V is at the P1 position and X is an amino acid at the P1' position. The preference is a function of both the binding affinity of the elastase for the cleavage site (K_M) and the rate of hydrolysis (k_{cat}). Hydrolysis by NE can also occur with other small hydrophobic amino acids at the P1 position but to a lesser degree (Zimmerman and Ashe, 1977). We tested the effect of mutating individual valines conservatively to glycines in the extracellular loops of α and γ ENaC because these subunits appear to be involved in activation and or processing by endogenous proteases (Masilamani et al., 1999; Hughey et al., 2004a; Ergonul et al., 2006; Knight et al., 2006). The valine mutation sites were chosen based on their proximity to previously implicated cleavage sites (Hughey et al., 2004a). A total of eight V to G mutants were evaluated, three in the α subunit and five in the γ subunits. Stable cell lines expressing these mutants were selected and the effects of aprotinin, NE, and trypsin on I_{Na} were measured. These results are summarized in Table I. All eight V to G mutants expressed baseline currents that were similar to wild-type hENaC-expressing cells. Furthermore aprotinin inhibited the baseline current to a similar degree and NE reversed this inhibition of I_{Na} (Table I). Only the double mutant $\alpha\beta\gamma_{V182G;V193G}$ was different from wild-type ENaC (WT). Unlike wild-type ENaC and several mutants where subsequent addition of trypsin had a minor further effect on I_{Na} following NE stimulation in aprotinin-treated cells (Table I, Fig. 4 B, and Fig. 5, A–D), $\alpha\beta\gamma_{V182G;V193G}$ could be substantially further stimulated by trypsin (Table I and Fig. 4, E and F). As shown in the figures, addition of NE to aprotinin-treated FRT cells expressing wild-type ENaC increased I_{Na} from 15.6 ± 0.86 μA/cm² to 27.8 ± 1.40 μA/cm² ($n = 36$) within 10 min. Thereafter, addition of trypsin caused only a small further increase to 31.3 ± 1.60 μA/cm². Thus NE caused an increase that was ~85% of the trypsin-induced maximal protease increase in wild-type ENaC-expressing cells. In contrast addition of NE to aprotinin-treated FRT cells expressing the $\alpha\beta\gamma_{V182G;V193G}$ mutant increased I_{Na} from 18.3 ± 0.67 to 25.9 ± 1.07 μA/cm² ($n = 39$), but the I_{SC} could be further stimulated to 39.9 ± 1.12 μA/cm² after the addition of trypsin. Thus in the $\alpha\beta\gamma_{V182G;V193G}$ cells, NE only stimulated ~36% of the I_{Na} stimulated by trypsin.

A closer examination of the current traces revealed that the rate of activation by NE was also affected by the valine to glycine mutations and this effect was investigated in greater detail. The changes in I_{Na} following addition of NE (300 nM) to wild-type and mutant ENaCs were monitored with time and reported (Fig. 6 A) as a fraction of the maximal trypsin-stimulated I_{Na}. The fractional current increase normalized to the maximum response after trypsin (ΔI_{PR}^{Norm}) was fitted to exponentials as described in Materials and methods to yield time constants. The ΔI_{PR}^{Norm} ~30 min after NE addition was taken as the measure of maximal NE-stimulated current. The fitted parameters are summarized in Table II for αβγ and the glycine scanning mutations showing that only specific mutations in the γ subunit appreciably

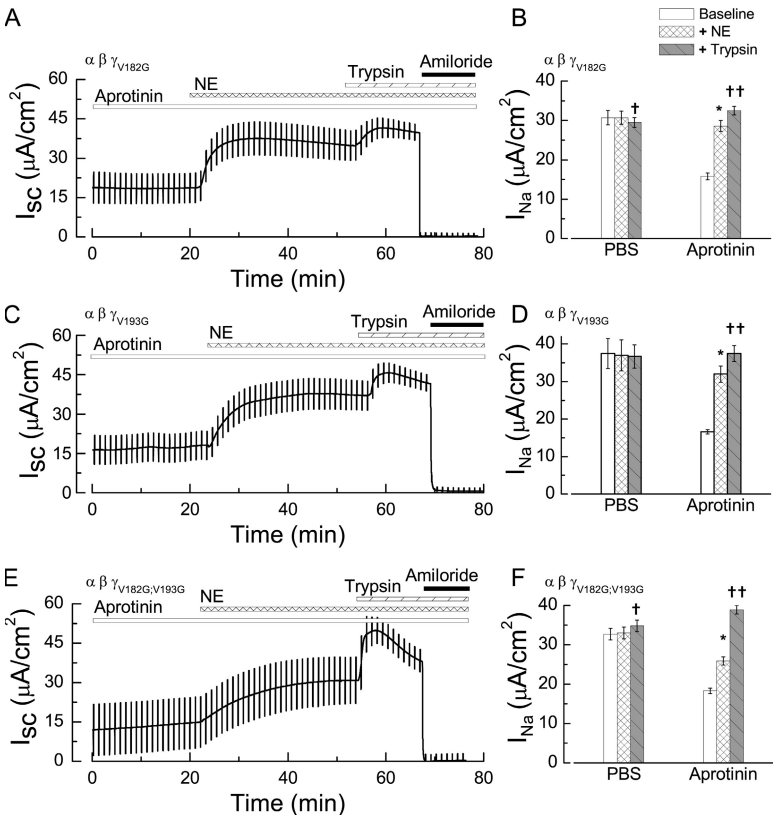

Figure 5. Two point mutations in γ ENaC inhibit NE activation of I_{Na} in FRT cells. (A) Representative I_{SC} of cells expressing γ_{V182G}, (C) γ_{V193G}, and (E) $\gamma_{V182G;193G}$ that were pretreated with 10 μM aprotinin before short circuiting. NE (300 nM) was added to the apical bath as indicated (horizontal bars). Subsequently, trypsin (15 μM) and amiloride (50 μM) were added. (B, D, and F) Mean (±SEM, n = 13–39) of baseline I_{Na} (open bars), I_{PR} (stripped bars), and I_{Tryp} (shaded bars) in cells pretreated with PBS or aprotinin that were expressing $\alpha\beta\gamma_{V182G}$ (B), $\alpha\beta\gamma_{V193G}$ (D), and $\alpha\beta\gamma_{V182G;193G}$ (F) mutants. *, $P < 0.05$ in Student's t test comparison of amiloride-sensitive I_{SC} before and after NE. †, $P < 0.05$; ††, $P < 0.01$ in Student's t test comparison of amiloride sensitive I_{SC} after NE and after trypsin.

change the time course. Representative time courses for wild type, $\alpha\beta\gamma_{V182G}$, $\alpha\beta\gamma_{V193G}$, and $\alpha\beta\gamma_{V182G;V193G}$ are shown in Fig. 5 A. In wild-type and $\alpha\beta\gamma_{V182G}$-expressing cells the $\Delta I_{PR}{}^{Norm}$ rose with identical rates and to similar plateau values with amplitudes 0.68 ± 0.05 and 0.64 ± 0.04, respectively. Therefore, mutating V182 to G had no effect on NE activation of current. The cells expressing $\alpha\beta\gamma_{V193G}$ had $\Delta I_{PR}{}^{Norm}$ of 0.53 ± 0.05, which was not significantly decreased from wild type; but they showed a significant elongation of the time constant from the wild-type value of 3.1 ± 0.18 min (n = 10) to 6.3 ± 0.36 min (n = 5). As noted above, cells expressing the double mutant, $\alpha\beta\gamma_{V182G;V193G}$, had a marked reduction of $\Delta I_{PR}{}^{Norm}$ (0.22 ± 0.02) as well as a further elongation of the time constant to 11.8 ± 1.49 min (n = 8). Therefore, while mutating the V182 to G182 had no discernible effect on its own, this mutation produced a pronounced effect in the presence of the already inhibitory V193G mutation. To differentiate an effect caused by changing a V from an effect introduced specifically by the G, several amino acids were substituted at positions 182 and 193. The effect of mutating γ V182 and V193 was not specific to glycine but consistent for several amino acid substitutions (S, T, D, E, and Q). Generally, substitutions at γ182 did not result in significant differences in the τ for the residues tested (Fig. 6). At residue 193, all the substitutions except E caused a significant prolongation of τ compared with wild type (Fig. 6 B). Substitutions at both γ182 and γ193 produced significant elongation of τ for all the substitutions compared with wild type (Fig. 6 B). The changes in $\Delta I_{PR}{}^{Norm}$ caused by the mutations were roughly consistent with the changes in τ. Generally, $\Delta I_{PR}{}^{Norm}$ was not affected by substitutions at γ 182 only, except with the S substitution (Fig. 6 C). The $\Delta I_{PR}{}^{Norm}$ was reduced for substitutions at γ 193, except for the G substitution (Fig. 6 C). All double substitutions at 182 and 193 resulted in decreased $\Delta I_{PR}{}^{Norm}$ compared with wild type. These results are more consistent with the conclusion that removal of a valine (as opposed to introduction of a specific residue) was responsible for both prolongation of τ and decreased $\Delta I_{PR}{}^{Norm}$. Secondarily, the conserved pattern where substitutions at 182 produce no effect; substitutions at 193 increased τ and decreased $\Delta I_{PR}{}^{Norm}$; and double substitutions further increasing τ and decreasing $\Delta I_{PR}{}^{Norm}$ suggest that the V193 is of primary importance in current activation by NE but V182 also has some effect unmasked in the absence of V193.

Identification of Elastase-specific Sites II: Porcine Pancreatic Elastase

First, we tested if the valines critical for NE were also critical for PE activation of current. I_{SC} following addition of PE (300 nM) was monitored to determine the effect of simultaneous substitutions at residues 182 and 193 on PE-mediated channel activation. The effects of the double substitutions on $\Delta I_{PR}{}^{Norm}$ were small compared with the results for NE. As shown in Fig. 7 (A and B),

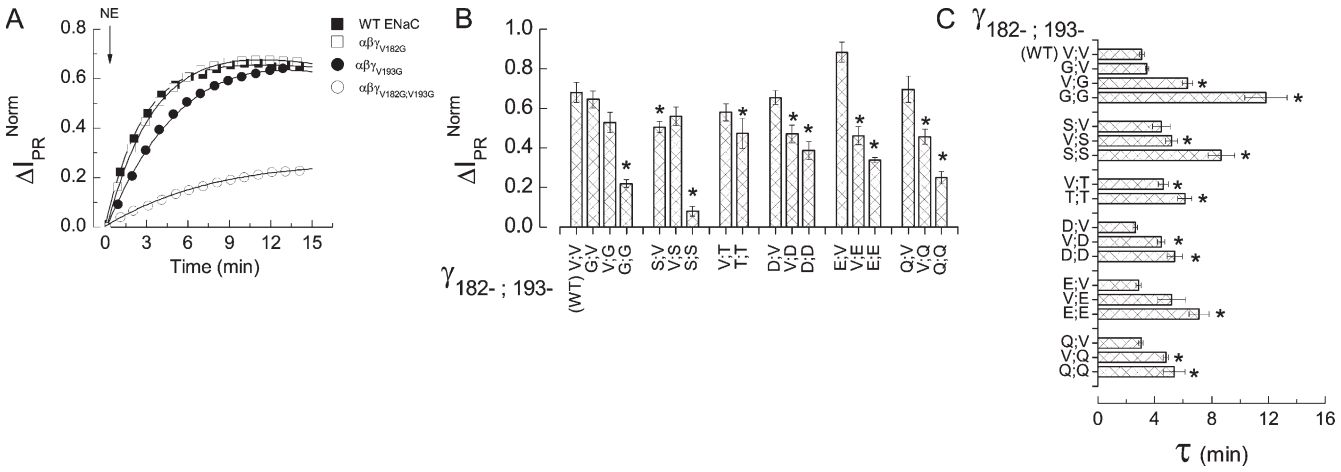

Figure 6. Effect of mutating residues 182 and 193 in the extracellular domain of γ ENaC on NE activation of I_{Na}. NE (300 nM) was added to short-circuited FRT cells expressing the indicated γ ENaC mutants that were pretreated with 10 μM aprotinin. 30 min after addition of NE, trypsin (15 μM) was added in excess over aprotinin to achieve a reference point for maximal protease stimulation. (A) Representative traces of $\Delta I_{PR}{}^{Norm}$ for NE activation of wild type (solid squares), $\alpha\beta\gamma_{V182G}$ (open squares), $\alpha\beta\gamma_{V193G}$ (solid circles), and $\alpha\beta\gamma_{V182G;\,193G}$ (open circles) ENaCs. The solid lines are the exponential fits of the data. (B) Steady-state values of $\Delta I_{PR}{}^{Norm}$ for the amino acid substitution at 182 and 193 in γ ENaC (mean ± SEM, n = 6–36). *, $P < 0.05$, one way ANOVA and t test comparison with wild type. (C) Summary of the τ from experiments described above (mean ± SEM, n = 4–10) for several amino acid substitutions at residues 182 and 193 in γ ENaC. *, $P < 0.01$, one way ANOVA.

the time courses for wild type and G substitutions were slightly prolonged. The τ was prolonged from 2.0 ± 0.14 min (n = 11) for wild type to 3.6 ± 0.27 min (n = 11) for the G substitutions. The effect on $\Delta I_{PR}{}^{Norm}$ was not different between wild type and G substitutions at ∼0.7 for both (n = 16 and 23, respectively; Fig. 7 C). The rest of the double substitutions examined (S, Q, E, and T) had small effects on τ and $\Delta I_{PR}{}^{Norm}$ (Fig. 7, D and E). These results show that the valines 182 and 193 were not critical for increasing I_{Na} by PE.

Unlike NE, the preferential residue at P1 is A for PE (Hartley and Shotton, 1971). Therefore one explanation for minor effects of the V substitutions is that PE interacts with the channel via its preferred residue somewhere else. We reasoned that γ A190 between the two valines critical for NE was a likely target. Substitution of the γ A190 to G resulted in significant attenuation of the current response to PE (Fig. 7, F–H). While 1,000 nM PE activated current in wild type and the $\alpha\beta\gamma_{V182G;V193G}$ double mutant ENaC (Fig. 7, F and G), with τ of 1.94 ± 0.12 and 2.17 ± 0.07 min, respectively, the mutant $\alpha\beta\gamma_{A190G}$ prevented PE activation of current. Because increases in I_{Na} were small to nonexistent in the $\alpha\beta\gamma_{A190G}$ mutant in response to PE, τ could not be resolved for all experiments. For those experiments where τ was resolved, it averaged 25.6 ± 1.09 min (Fig. 7 H). Furthermore, the $\Delta I_{PR}{}^{Norm}$, which was 0.70 ± 0.04 and 0.89 ± 0.03 for wild type and $\alpha\beta\gamma_{V182G;V193G}$, respectively, was reduced to 0.26 ± 0.02 for $\alpha\beta\gamma_{A190G}$ (Fig. 7 I). These results are consistent with γ A190 being of primary significance for PE current stimulation, whereas the Vs are more important for NE current stimulation. Because the results are consistent with the P1 preferences for PE and NE, they suggest that these enzymes interact with the channel according to their substrate recognition specificities.

Concentration Dependence of Protease Activation

Because the previous results suggest direct protease–ENaC interaction, a concentration dependence of activation was used to delineate two mechanistic possibilities of current activation: (1) that direct binding was sufficient for channel activation or (2) that binding plus a secondary step is necessary. As can be seen from the

TABLE II

Fitted Parameters for Neutrophil Elastase Activation of ENaC-mediated Na^+ Current in WT and Mutant ENaC Heterologously Expressed in FRT Cells

Construct	τ (±SEM)	$\Delta I_{PR}{}^{Norm}$ (±SEM)	***n*** (filters)
	min		
WT	3.10 ± 0.18	0.68 ± 0.05	10
α-V171G	1.52 ± 0.155[a]	0.96 ± 0.03	6
α-V193G	1.94 ± 0.061	0.85 ± 0.07	6
α-V206G	2.24 ± 0.416	0.74 ± 0.03	3
γ-V110G	1.89 ± 0.748	0.96 ± 0.05	3
γ-V110/146G	1.80 ± 0.390	0.89 ± 0.04	5
γ-V182G	3.46 ± 0.17	0.64 ± 0.05	8
γ-V193G	6.32 ± 0.36[a]	0.53 ± 0.05	8
γ-V182/193G	11.82 ± 1.49[a]	0.22 ± 0.02[a]	8
γ-V201G	3.95 ± 0.810	0.79 ± 0.030	8

Values are the mean of the individual fits from n experiments.
[a]$P < 0.05$ ANOVA unpaired t test comparison with WT values.

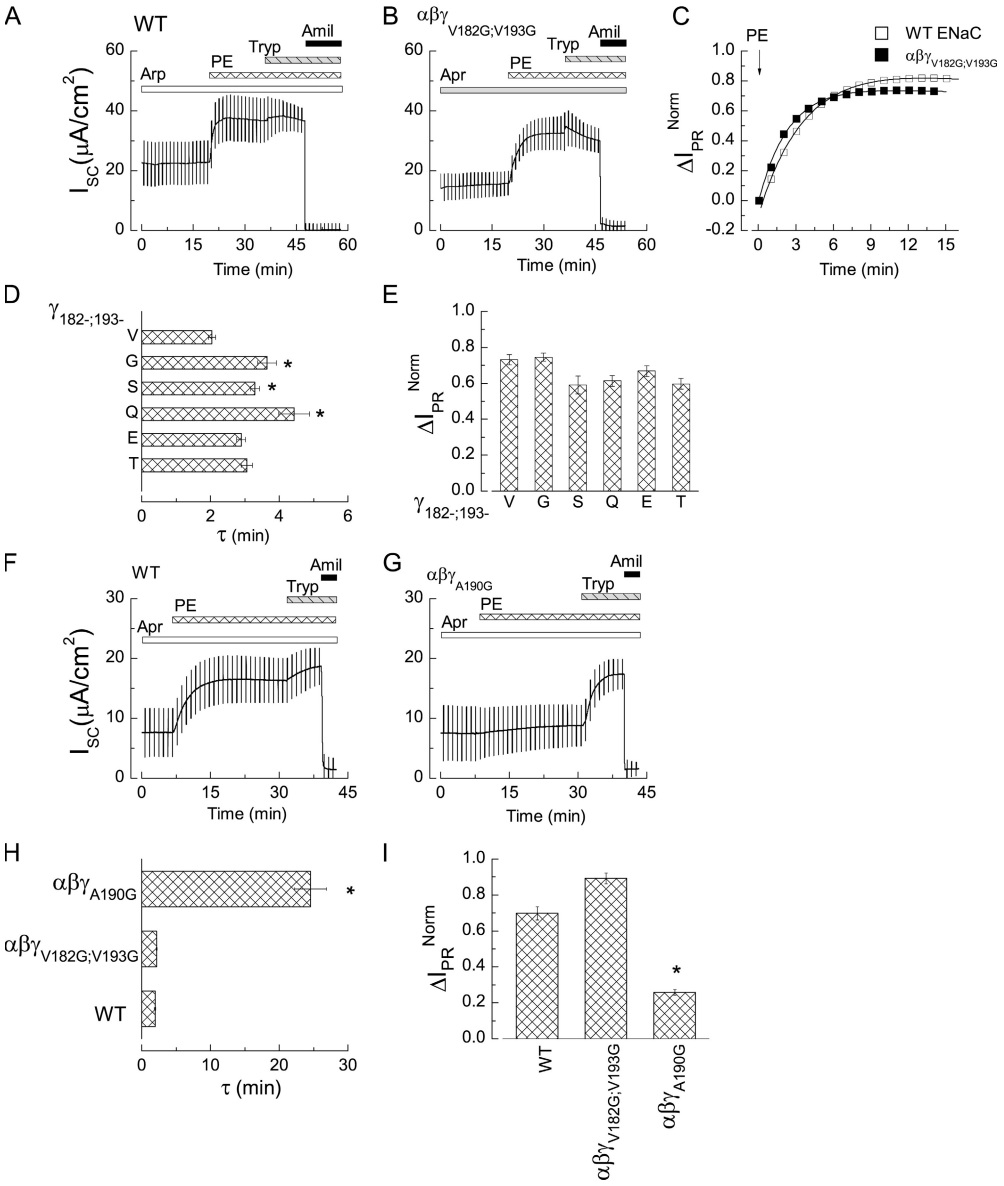

Figure 7. Effect of mutations at 182, 190, and 193 in the extracellular domain of γ ENaC on PE activation of I_{Na^+}. PE (300 nM) was added to short-circuited FRT cells expressing the indicated γ ENaC mutants that were pretreated with 10 μM aprotinin. 20 min after addition of PE, trypsin (15 μM) was added in excess over aprotinin to achieve a reference point for maximal protease stimulation. (A and B) Representative I_{SC} trace of FRT cells expressing wild type or $\alpha\beta\gamma_{V182G;V193G}$ mutant. (C) Representative $\Delta I_{PR}{}^{Norm}$ response to PE for wild type (solid squares) and $\alpha\beta\gamma_{V182G;V193G}$ (open squares) mutant with exponential fits (solid lines). (D) Summary of the τ (±SEM, n = 4–11) from experiments described above for double substitutions at residues 182 and 193 in γ ENaC. (E) The steady-state $\Delta I_{PR}{}^{Norm}$ (±SEM, n = 8–23) ratios for the double substitutions at 182 and 193 in γ ENaC. (F and G) Representative I_{SC} trace for FRT cells expressing wild type, $\alpha\beta\gamma_{V182G;V193G}$, and $\alpha\beta\gamma_{A190G}$ ENaC, respectively. 1,000 nM PE was used. (H and I) τ (±SEM, n = 5–8) and steady-state $\Delta I_{PR}{}^{Norm}$ (±SEM, n = 5–8) for responses to 1,000 nM PE in cells expressing wild type (open bars), $\alpha\beta\gamma_{V182G;193G}$ (light gray bars), and $\alpha\beta\gamma_{A190G}$ (dark gray bars). *, $P < 0.05$, one way ANOVA and t test comparison with wild type.

progress curves of $\Delta I_{PR}{}^{Norm}$ (Fig. 8 A) the rates of current activation as well as the amplitudes of the increase were concentration dependent. Increasing NE concentration from 30 to 1,000 nM reduced τ for cells expressing wild type from 11.3 ± 1.5 min (n = 8) to 1.6 ± 0.04 min (n = 8). The $\Delta I_{PR}{}^{Norm}$ increased with increasing concentration of NE from 0.22 ± 0.02 at 30 nM to 0.75 ± 0.05 at 1,000 nM (Fig. 8 D). The τ and $\Delta I_{PR}{}^{Norm}$ for cells expressing the $\alpha\beta\gamma_{V182G;\,V193G}$ mutant were also concentration dependent (Fig. 8, B and D). Time constants decreased from 13.8 ± 3.2 min (n = 8) at 30 nM NE to 5.9 ± 0.3 min (n = 8) at 1,000 nM NE, and $\Delta I_{PR}{}^{Norm}$ increased from −0.02 ± 0.04 to 0.52 ± 0.02. The concentration dependence of current activation suggests a first approximation of the mechanism of activation of current by NE and PE. Because only one exponential component was present in the fitting of the time courses, the reciprocal of the derived time constants were taken as a pseudo-first-order rate coefficient, k_{obs}. For wild-type ENaC, the pseudo-first-order rate constant (k_{obs}) showed saturation behavior with respect to the added enzyme concentration (Fig. 8 C). From the saturation at relatively slow rates, assuming that the enzyme concentration in the chamber was not altered by concentration-dependent autolysis and that the enzyme concentration is in a large excess over its target ENaC, apparent kinetic parameters were derived based on Eq. 8 by nonlinear regression of k_{obs} against the added enzyme concentration.

In cells expressing wild-type ENaC the K_M was 570 ± 240 nM NE and the k_{cat} was 14.4 ± 2.11 × 10^{-3} s^{-1}. When the $\alpha\beta\gamma_{V182G;V193G}$ was expressed, the k_{obs} also showed a dependence on enzyme concentration (Fig. 8, B–D). However, the dependence of k_{obs} on enzyme

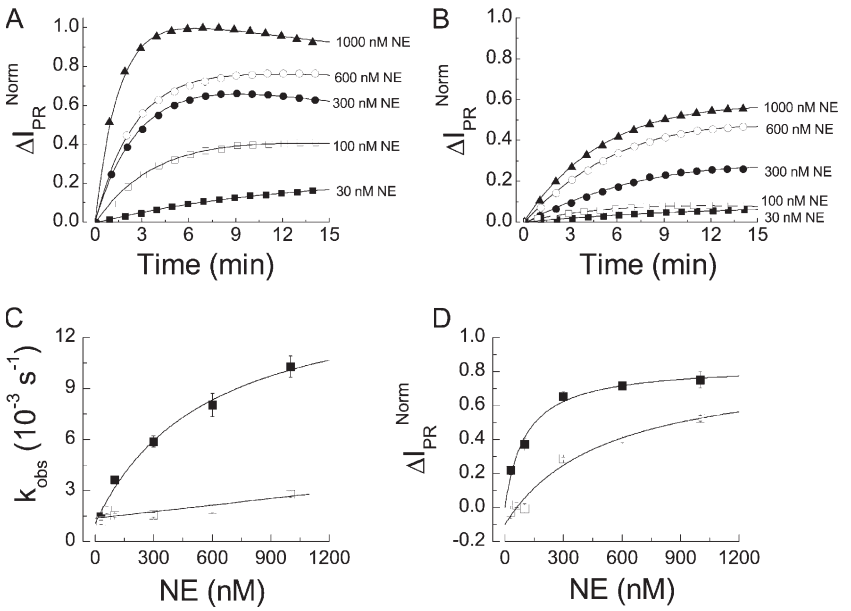

Figure 8. NE concentration dependence of the activation of I_{Na} in FRT cells expressing wild type and $\alpha\beta\gamma_{V182G;V193G}$ mutant ENaC. (A) Representative $\Delta I_{PR}{}^{Norm}$ responses in FRT cells expressing wild-type ENaC to 30 nM NE (solid squares), 100 nM NE (open squares), 300 nM NE (solid circles), 600 nM NE (open circles), and 1,000 nM NE (solid triangles). (B) Representative $\Delta I_{PR}{}^{Norm}$ responses in FRT cells expressing $\alpha\beta\gamma_{V182G;V193G}$ to 30 nM NE (solid squares), 100 nM NE (open squares), 300 nM NE (solid circles), 600 nM NE (open circles), and 1,000 nM NE (solid triangles). (C) Mean (±SEM, n = 7–8) of k_{obs} ($=1/\tau$) with respect to the NE concentration for FRT cells expressing wild type (solid squares) and $\alpha\beta\gamma_{V182G;V193G}$ (open squares) ENaC. The solid line through the solid squares is the predicted values from a fit of the wild-type dataset to a kinetic model (see Results) were k_{cat} = 14.2 10^{-3} s^{-1} and K_M = 570 nM. The solid line through the open squares is a linear regression of the $\alpha\beta\gamma_{V182G;V193G}$ dataset with slope 1,300 $M^{-1}s^{-1}$ ($P < 0.05$). (D) Steady-state $\Delta I_{PR}{}^{Norm}$ (±SEM, n = 7–8) ratios for wild type (solid squares) and $\alpha\beta\gamma_{V182G;193G}$ mutant (open squares). Solid lines are fits of the datasets to saturation kinetics. $K_{1/2}$ was 89 and 470 nM, respectively.

concentration, in contrast to wild-type ENaC, did not show an apparent saturation; consequently the parameters k_{cat} and K_M could not be calculated. One reason why this arises may be because the concentration of NE used was well below the K_M. A linear regression was performed under the assumption that $[E] << K_M$. The slope of the regression, k_{cat}/K_M, was 1,300 ± 200 × $M^{-1}s^{-1}$. This quotient represents the efficiency of NE activation of the $\gamma_{V182G;V193G}$ double mutant. This quotient for wild-type ENaC was calculated from the fitted parameters and was ~25,000 $M^{-1}s^{-1}$. Thus NE efficiency for activating wild-type ENaC is ~20 times that for activating the $\alpha\beta\gamma_{V182G;V193G}$ mutant. The $\Delta I_{PR}{}^{Norm}$ current plateau values at each NE concentration were also fitted to a saturation curve of the form

$$\Delta I_{PR}{}^{\mathrm{Norm}} = \frac{(\Delta I_{PR}{}^{Norm})^{\max}\ [E]}{K_{1/2} + [E]},$$

where $(\Delta I_{PR}{}^{Norm})^{max}$ is the maximum increase and $K_{1/2}$ is the enzyme concentration at half maximal stimulation. For NE on wild-type ENaC the $K_{1/2}$ was 100 ± 18 nM, and $(\Delta I_{PR}/I_{Tryp})^{Max}$ was 0.84 ± 0.04. For NE on the $\alpha\beta\gamma_{V182G;V193G}$ mutant, $K_{1/2}$ was 510 ± 162 nM and $(\Delta I_{PR}{}^{Norm})^{Max}$ was 0.94 ± 0.14. Consequently, the apparent affinity for NE activation of I_{Na} is ~5-fold weaker for the $\alpha\beta\gamma_{V182G;193G}$ mutant compared with wild-type ENaC.

A concentration dependence of activation was also observed for PE activation of the I_{Na}. The same analysis as described above was performed for the PE datasets. For wild-type ENaC, the saturation behavior of the activation rate (Fig. 9 A) had a K_M of 204± 140 nM and k_{cat} was 11.4 ± 1.34 × 10^{-3} s^{-1}. For the mutant $\alpha\beta\gamma_{V182G;V193G}$, the dependence of k_{obs} on PE concentration was well defined, in contrast to what was observed for NE. Unlike NE's effect on this mutant, there was saturation with PE demonstrating a K_M of 290 ± 51 nM and a k_{cat} of 8.7 ± 0.39 × 10^{-3} s^{-1}. Therefore, unlike for NE activation of I_{Na} these mutations had a minimal effect on PE activation of I_{Na}. The parameters for the $\Delta I_{PR}{}^{Norm}$ versus concentration were $K_{1/2}$ of 77 ± 30 nM and 35 ± 9.2 nM for both wild type and $\alpha\beta\gamma_{V182G;V19G}$, respectively, and $(\Delta I_{PR}{}^{Norm})^{Max}$ were 0.7 ± 0.2 and 1 ± 0.05, respectively. Clearly for both wild type and $\alpha\beta\gamma_{V182G;V193G}$, activation saturation occurred at low enzyme concentrations (Fig. 8 B) and no difference could be discerned between the two constructs. In contrast to these minor effects, the concentration dependence of PE activation of I_{Na} in the $\alpha\beta\gamma_{A190G}$ mutant was significantly impaired. The k_{obs} increased slowly with enzyme concentration, showing no apparent saturation (Fig. 9 A). Linear regression gave k_{cat}/K_M of ~550 $M^{-1}s^{-1}$. Thus PE activation of wild-type ENaC was ~100-fold more efficient than PE activation of $\alpha\beta\gamma_{A190G}$. This loss in efficiency is accompanied by a 15-fold increase of the $K_{1/2}$ for $\Delta I_{PR}{}^{Norm}$ to 1,140 nM (Fig. 9 B).

NE and PE Cleavage of the γ ENaC Segment

Next NE and PE were evaluated for their ability to cleave the identified region of γ ENaC and the specific

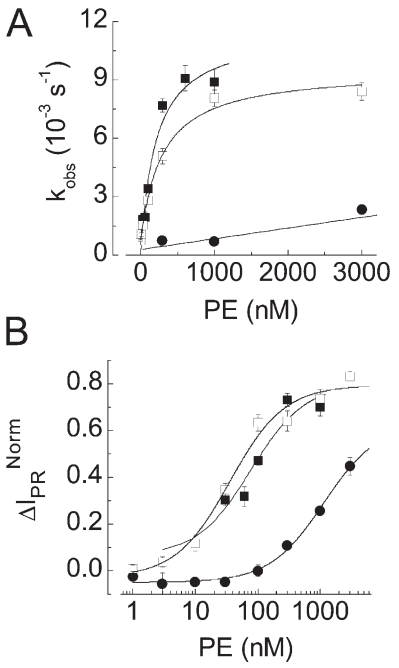

Figure 9. PE concentration dependence of the activation of I_{Na} in FRT cells expressing wild type, $\alpha\beta\gamma_{V182G;V193G}$ mutant, or $\alpha\beta\gamma_{A190G}$ ENaC. (A) Mean (±SEM, $n = 8$) of k_{obs} with respect to the PE concentration for FRT cells expressing wild type (solid squares) and $\alpha\beta\gamma_{V182G;V193G}$ ENaC (open squares), and $\alpha\beta\gamma_{A190G}$ ENaC (solid circles). The solid lines are the kinetic fits of the data as described in Materials and methods; fitted parameters k_{cat} and K_M were 11.4×10^{-3} s^{-1} and 204 nM for wild-type ENaC; 8.7×10^{-3} s^{-1} and 294 nM for $\alpha\beta\gamma_{V182G;V193G}$. Linear regression of the k_{obs} versus PE concentration for $\alpha\beta\gamma_{A190G}$ gave a slope of 550 ± 89 $M^{-1}s^{-1}$ ($P < 0.05$). (D) $\Delta I_{PR}{}^{Norm}$ (mean ± SEM, $n = 8$) ratios for wild type (solid squares) and $\alpha\beta\gamma_{V182G;V193G}$ (open squares) mutant. Solid lines are fits to saturation kinetics. $K_{1/2}$ was 77 ± 35, 35 ± 9.2, and 1140 ± 221 nM, respectively.

proteolytic sites were determined by MALDI-TOF mass spectrometry. The peptide T^{176}-S^{198} (200 μM), corresponding to the amino acid sequence T176 to S198 of the γ ENaC subunit, was incubated with 200 nM NE or PE in tris-acetate buffer. MALDI-TOF mass spectrometry showed the undigested peptide T^{176}-S^{198} at m/z of 2546.6 D. Incubation of peptide T^{176}-S^{198} with NE for 5 min resulted in a new peak at 1950.9 D corresponding to the molecular weight of peptide T^{176}-V^{193} as well as a new peak at 615.3 D corresponding to the peptide M^{194}-S^{198} along with undigested full-length peptide at 2547.1 D (Table III). Mass spectrometry of the PE digest showed the appearance of new peaks at 1650.8 D and 915.2 corresponding to peptides T^{176}-A^{190} and S^{191}-S^{198}, respectively (Table III). These fragments indicated that NE hydrolyzed the peptide between V193 and M194 primarily, whereas PE hydrolyzed the peptide between A190 and S191. Cleavages at the specific sites were detected within 1 min of incubation. After prolonged incubation with NE (30 min), a peak at 886.0 D corresponding to the peptide T^{176}-V^{182} was also evident but minor, suggesting that cleavage by NE can occur between V182 and G183 but is not efficient. Substitution of V182 and V193 with glycines prevented cleavage of the peptide by NE and glycine substitution of A190 prevented cleavage by PE. Consequently, a peptide with a sequence contained within γ ENaC can be cleaved by NE and PE at the cleavage sites corresponding to the residues that mediate channel activation by the enzymes.

Thrombin Activation of ENaC

To further investigate the idea that channel activation could be mediated by protease ENaC interaction at the sequence between γ182 and γ193, the γ 186 to 190 sequence (IIHKA) was changed to γ 186…LVPRG to give the mutant $\alpha\beta\gamma_{Th}$. The LVPRGS sequence matches the specific thrombin consensus sequence of bovine factor XIII (Takagi and Doolittle, 1974) where thrombin cleaves after R and is often used for cleavage of fusion proteins (Jenny et al., 2003). Aprotinin is not known to inhibit thrombin (Scott et al., 1987; Auerswald et al., 1988; Pintigny and Dachary-Prigent, 1992). Human α thrombin (TH), in contrast to NE and PE, did not elicit significant current increases in FRT cells expressing wild-type ENaC, which were aprotinin pretreated (Fig. 10, A and C). The baseline I_{Na} (9.8 ± 1.44 μA/cm^2) was not significantly increased after 300 nM TH (11.5 ± 0.91 μA/cm^2) but subsequent trypsin addition increased I_{Na} to 23.7 ± 0.65 μA/cm^2 ($n = 8$). For cells expressing $\alpha\beta\gamma_{Th}$, 300 nM TH elicited rapid current increases (Fig. 10, B–D) as did 300 nM NE. On average, TH increased I_{Na} from a baseline of 14.3 ± 1.32 to 23.8 ± 1.17 μA/cm^2, which was not significantly further increased by trypsin addition (24.9 ± 0.72 μA/cm^2; $n = 8$). FPR-chloromethyl ketone completely prevented the stimulation of I_{Na} by thrombin (ΔI_{Na} with inhibitor −1.5 ± 1.18 μA/cm^2, $n = 6$). A comparison of the $\Delta I_{PR}{}^{Norm}$ (Fig. 10 D) showed that while NE and PE activated wild-type ENaC (0.6 ± 0.02 and 0.7 ± 0.01, $n = 8$–16), TH had only a small effect (0.1 ± 0.02, $n = 4$). On the other hand TH activated $\alpha\beta\gamma_{Th}$ ($\Delta I_{PR}{}^{Norm} = 0.9 \pm 0.02$, $n = 8$) as did NE ($\Delta I_{PR}{}^{Norm} = 0.7 \pm 0.04$, $n = 4$). Interestingly, while NE also activated $\alpha\beta\gamma_{Th}$, activation of $\alpha\beta\gamma_{Th}$ by PE was significantly impaired (0.2 ± 0.04, $n = 4$). This result was consistent with the change of γ190A to G, which previously led to inhibited responses to PE. The activation of $\alpha\beta\gamma_{Th}$ by thrombin was similar to activation of wild-type ENaC by NE and PE, showing a concentration dependence of both the k_{obs} and steady-state $\Delta I_{PR}{}^{Norm}$ (Fig. 10, E and F). The k_{cat} was 10.1 ± 0.13 × 10^{-3} s^{-1}, K_M was 340 ± 19.5 nM, and $K_{1/2}$ was 14.8 ± 1.98 nM. Thrombin did not cleave the wt T^{176}- S^{198} peptide but did cleave the peptide substituted with a thrombin consensus sequence (Table III). In vitro translation studies of αβ hENaC together with wt γ or γ_{Th} revealed thrombin cleavage of γ_{Th} but not wt γ (Fig. 11). In vitro translation of γ hENaC yielded two bands, one at 74 kD and

TABLE III

Peptide Products Derived from a Segment of Human γ ENaC after Protease Digestion and Analysis by MALDI-TOF Mass Spectrometry

Substrate	Protease	Observed Mass (m/z)	Calculated Mass (m/z)	Cleavage Site (↓)
WT-γ	–	2546.6	2546.8	TGRKRKVGGSIIHKASNVMHIES
	NE	2547.1, 1950.9, 615.3	2546.8, 1950.2, 615.0	TGRKRKVGGSIIHKASNV↓MHIES
	PE	2546.7, 1649.5, 915.2	2546.8, 1649.8, 915.0	TGRKRKVGGSIIHKA↓SNVMHIES
	TH	2546.6	2546.8	TGRKRKVGGSIIHKASNVMHIES
V182G;V193G-γ	–	2418.7	2419.8	TGRKRKGGGSIIHKASNGMHIES
	NE	2418.7	2419.8	TGRKRKGGGSIIHKASNGMHIES
A190G-γ	–	2488.9	2489.9	TGRKRKVGGSIIHKGSNVMHIES
	PE	2488.9	2489.9	TGRKRKVGGSIIHKGSNVMHIES
TH-γ	–	2464.4	2463.9	TGRKRKVGGSLVPRGSNVMHIES
	TH	1511.4, 973.2	1510.8, 972.4	TGRKRKVGGSLVPR↓GSNVMHIES

Substrate, WT-γ (Ac- ^{176}TGRKRKVGGSIIHKASNVMHIES^{198}-$CONH_2$),was derived from the γ hENaC subunit and amino acid residues substituted as indicated to yield the respective peptides: V182G;V193G-γ TGRKRKGGGSIIHKASNGMHIES; A190G-γ TGRKRKVGGSIIHKGSNVMHIES and TH-γ TGRKRKVGGSLVPRGSNVMHIES. Peptides (200 μM) were incubated with vehicle (–) or 200 nM proteases (NE, human neutrophil elastase; PE, porcine pancreatic elastase; TH, human α thrombin) in Tris-acetate buffer (pH 7.4) at 37°C for 5 min, respectively. The reaction was stopped by the addition of 1% TFA.

one at 82 kD. Treatment of γ_{Th} with thrombin resulted in the appearance of a lower mass C-terminal band at 53 kD. The lower mass band at 53 kD is the expected size for cleavage of γ_{Th} at R189 in the thrombin consensus sequence. These results demonstrate thrombin can cleave γ_{Th} and this cleavage may mediate channel activation. Several attempts were made to detect a thrombin-liberated γ fragment in $\alpha\beta V_{th}$-expressing FRT cells. However the results from these studies were negative and we believe due to the low abundance of ENaC expression in our stable FRT cell lines.

DISCUSSION

The studies reported here were made possible by the development of a tripromoter plasmid expressing all three human ENaC subunits (hENaC). Cell lines stably expressing wild-type and mutant ENaC could be selected using a single antibiotic. FRT cells were chosen because they are readily transfected, do not express any native rat ENaC, and form a moderately tight epithelium (1–2 $k\Omega cm^2$). Previous studies in FRT cells using three separate ENaC subunit plasmids have shown ENaC is targeted to the apical membrane, allowing one to use standard transepithelial short circuit current (I_{SC}) measurements to study channel activity (Snyder, 2000; Snyder et al., 2004; Knight et al., 2006). Our studies reveal hENaC-FRT cells respond to aldosterone and dexamethasone treatment in a manner similar to native ENaC expressing epithelia (Garty and Palmer, 1997). Dexamethasone-treated hENaC-FRT cells provided robust I_{Na} that were aprotinin inhibited and exogenous protease activated. We used dexamethasone treated, aprotinin-inhibited hENaC-FRT cells to investigate the mechanism of channel activation by exogenous protease. The preponderance of evidence, including functional measurements of I_{Na} responses to proteases, mutational analysis, kinetic analysis of protease concentration and time-dependent responses, mass spectrometry of peptide cleavage products, and thrombin cleavage of γ_{Th} ENaC, support the conclusion that exogenous proteases directly interact with the γ subunit to cause channel activation and that channel activation may involve cleavage of the γ subunit.

Approximately 50% of the I_{Na} in the hENaC-FRT cells was inhibited by the serine protease inhibitor aprotinin. A similar aprotinin inhibitory effect on I_{Na} of 50–80% has been observed in a number of epithelia that natively express ENaC and includes the following: toad urinary bladder (Margolius and Chao, 1980; Orce et al., 1980) amphibian (Vallet et al., 1997; Adebamiro et al., 2005) and murine (Nakhoul et al., 1998; Liu et al., 2002) renal epithelia, and human bronchial (Bridges et al., 2001; Myerburg et al., 2006) nasal (Donaldson et al., 2002), and alveolar (Planes et al., 2005) epithelia. One may infer from these observations that there exists an endogenous aprotinin-sensitive protease responsible for ENaC activation. Support for this notion comes from the cloning of several membrane proteases that when coexpressed with ENaC cause channel activation (Vallet et al., 1997; Vuagniaux et al., 2002; Andreasen et al., 2006). The inhibitory effects of aprotinin on I_{Na} can be reversed by aprotinin washout or by the addition of excess exogenous proteases such as trypsin and elastase and this too was observed in the hENaC-FRT cells. The aprotinin effect is consistent with the notion that activation of channels by proteases at the apical membrane is blocked by aprotinin, producing a time-dependent reduction of the number of active channels (Adebamiro et al., 2005) that results from internalization or degradation of already activated channels. Channels newly arriving at the apical membrane then form a pool that can be activated by exogenous proteases. It was recently shown that a more substantial increase in current by

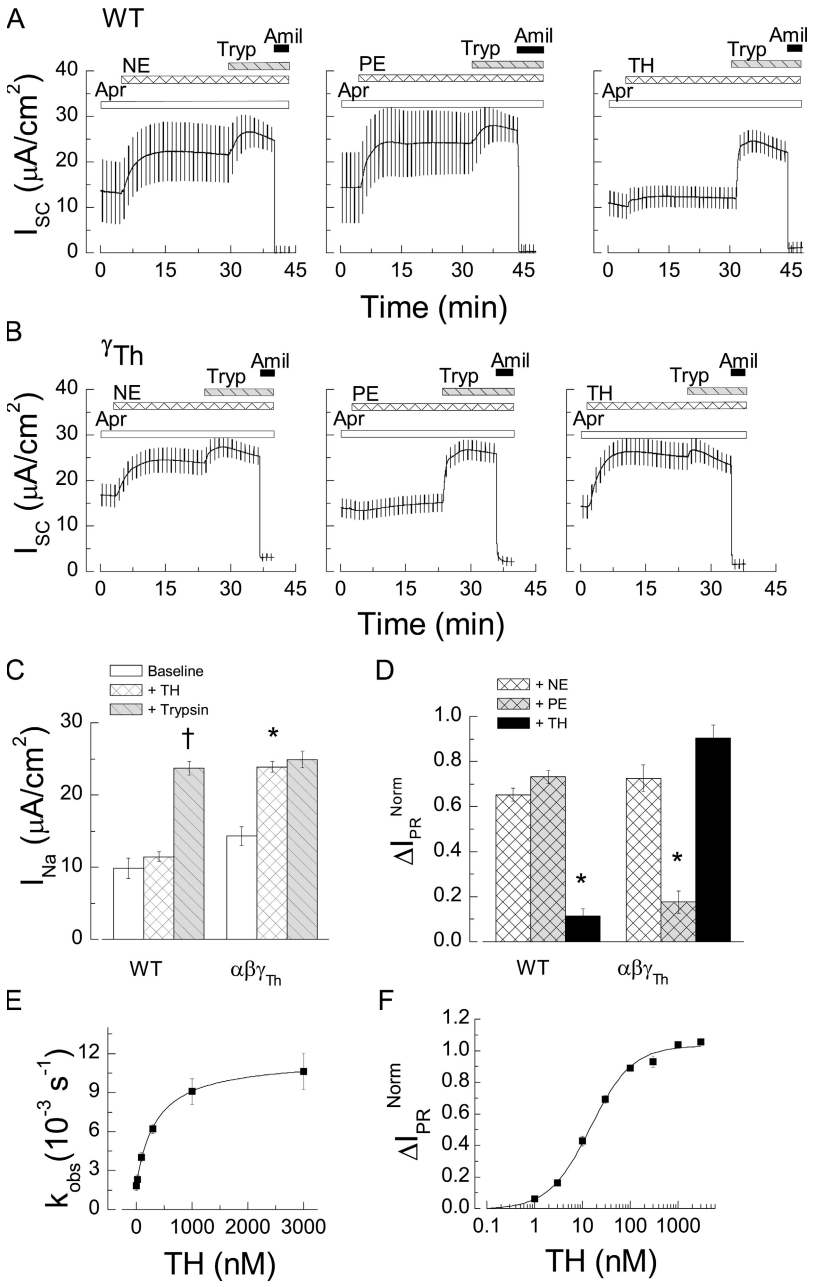

Figure 10. Thrombin-dependent activation of I_{Na} achieved by insertion of a thrombin recognition sequence. (A) Addition of NE, PE, and TH (300 nM) to FRT cells expressing wild-type ENaC or (B) FRT cells expressing $\alpha\beta\gamma_{Th}$ (γ186…iihka→γ186…lvprg) ENaC pretreated with aprotinin (10 μM) for the indicated period. Trypsin (15 μM) and amiloride (50 μM) were added as indicated. (C) I_{Na} (mean ± SEM, $n = 8$) in FRT cells expressing wild type and $\alpha\beta\gamma_{V182G;V193G}$ at baseline (open bars) and subsequent to 300 nM TH (hatch bars) and 15 μM Trypsin (stripped bars). *, $P < 0.05$, *t* test comparison of I_{Na} at baseline with I_{Na} after TH; †, $P < 0.01$, *t* test comparison of I_{Na} after TH with I_{Na} after trypsin. (D) Summary of the effect of NE (open bars), PE (gray bars), and TH (black bars) on wild type and $\alpha\beta\gamma_{Th}$ ENaC as measured by ΔI_{PR}^{Norm} (mean ± SEM, $n = 8$). *, $P < 0.05$, one way ANOVA and *t* test comparison with wild type. (E) The concentration dependence of k_{obs} (mean ± SEM, $n = 5$) and (F) ΔI_{PR}^{Norm} (mean ± SEM, $n = 5$) for TH activation of current for $\alpha\beta\gamma_{Th}$. Solid lines are fits to the data as described in Materials and methods. Parameters k_{cat} and K_M were 10.1×10^{-3} s^{-1} and 340 nM. The half maximal concentration for ΔI_{PR}^{Norm} was 15 nM.

exogenous trypsin could be seen in transiently transfected FRT cells expressing ENaC (Knight et al., 2006) unlike the small increases we observed. The difference may result from our use of stably transfected cells with a long incubation period on filters. In the studies reported here we used the hENaC-FRT cells and site-directed mutagenesis of hENaC together with the amino acid preferences of NE and PE to determine whether there is a direct interaction between ENaC and proteases in the channel activating process.

There are several possible mechanisms whereby the aprotinin inhibition of I_{Na} can be reversed by exogenous proteases in FRT cells. The binding of aprotinin by the proteases can be ruled out since the concentrations of proteases that activate I_{Na} are much less than the aprotinin concentration and insufficient to form an aprotinin sink. In other systems such as *Xenopus* oocytes and fibroblasts, activation by trypsin and NE can be seen in the absence of aprotinin. Protease-dependent effects on trafficking are possible but unlikely given the observations that trypsin did not increase cell surface quantities of channel subunits (Chraibi et al., 1998) and trypsin is able to activate current in excised outside-out membrane patches (Caldwell et al., 2004). A role for trafficking is also unlikely based on the mutational studies reported here and discussed below, indicating that the activation requires binding. The activation of ENaC by extracellular proteases may result from protease

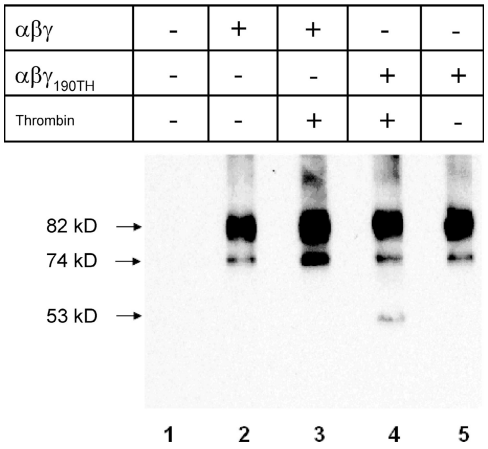

Figure 11. Thrombin cleavage of the γ_{Th} subunit but not the wt-γ subunit. Wild type αβhENaC plus wt-γ or γ_{Th} hENaC cDNAs were transcribed and translated in vitro in the presence of microsomes. Microsomes were pelleted, lysed, and treated with buffer or 200 nM thrombin for 5 min. Samples were run on SDS-PAGE and probed by Western blot with an anti-V5 antibody targeting a V5 epitope on the C terminus on the γ subunit. Lane 1, negative control without ENaC cDNA; lanes 2 and 3, with wt αβγ hENaC cDNA; lanes 4 and 5 with $\alpha\beta\gamma_{Th}$ hENaC cDNA. Samples in lanes 3 and 4 were treated with 200 nM thrombin. In vitro translation of αβγ hENaC yielded two major bands at 82 and 74 kD. Thrombin treatment of the $\alpha\beta\gamma_{Th}$ hENaC produced a lower mass band at 53 kD as expected for cleavage of the γ subunit at R189. The 53-kD band was not observed in thrombin treated wt αβγ ENaC samples. These results are representative of three similar experiments.

interaction with a protease responsive receptor which subsequently activates ENaC or from a direct protease interaction with ENaC. A requirement for a diffusible second messenger has not yet been identified for the protease dependent activation and in particular signaling through G proteins via protease-activated receptors did not appear to be necessary (Chraibi et al., 1998; Caldwell et al., 2004; but see Bengrine et al., 2007). Since it is possible that nonaqueous lipids or localized protein–protein interactions may transduce the protease signal, direct and indirect mechanisms remain distinct possibilities explaining channel activation by proteases.

There are several lines of evidence suggesting a direct protease interaction with the channel. The large extracellular domain (70%) of the ENaC/DEG family of ion channels suggests that extracellular ligand and protein–protein interactions may play a role in the physiology of these channels. Such interactions have been identified for the degenerin members of the family (Tavernarakis and Driscoll, 1997). In this report we identified a segment in the γ subunit that is involved in elastase-dependent activation of the channel. This segment is in the extracellular domain just after the first membrane-spanning domain (M1). The post-M1 region has been implicated in endogenous furin cleavage of γ ENaC and exogenous trypsin cleavage of ASIC1a, a member of the ENaC superfamily of ion channels (Hughey et al., 2004a; Vukicevic et al., 2006). The idea that the post-M1 region of γ ENaC is accessible is supported by the ability to label cell surface ENaC with antibodies directed against this region (Firsov et al., 1996). Cleavage of ASIC1a changes the pH dependence of channel gating (Poirot et al., 2004). Furin cleavage and trypsin activation of ENaC appear to modulate Na^+ dependence of channel gating (Chraibi and Horisberger, 2002; Sheng et al., 2006). The segment identified is therefore in an accessible part of the channel that is involved in channel regulation. A scanning mutagenesis, changing the likely primary amino acid position based on the specificity of NE identified two residues in γ ENaC critical for NE-dependent activation of ENaC. Substitutions at γV182 and γV192 specifically inhibited the activation of ENaC by NE; because neither PE, a similar protease, nor trypsin activation was significantly affected. Since the substitutions did not inhibit activation by PE and trypsin and did not affect endogenous protease activation (implied by the equivalent control currents and aprotinin sensitivity for wild-type and mutant ENaC) the substitutions did not impinge upon a common protease activation pathway. The specificity provides evidence that NE interacts directly with ENaC since interaction of proteases with a different receptor that subsequently activates ENaC would result in significant cross-interaction by virtue of ENaC being the final common step in such a pathway. The results show that one residue, γA190, in the vicinity of the residues critical for NE subserves PE-dependent activation of ENaC. As observed for NE, the effect is also specific since NE and trypsin activated the γA190G mutant channels. Furthermore, in the context of the $\alpha\beta\gamma_{Th}$ construct the specificity of γA190 for PE was evident since this construct with intact γV182 and γV193 residues but with a γA190G mutation was activated by NE and TH but PE activation was impaired. The presence of a sequence recognized by the thrombin active site creates a gain of function whereby the channel, not naturally activated by thrombin, becomes a thrombin-activated channel. When the thrombin catalytic site is blocked by FPR-chloromethyl ketone, thrombin no longer activates the channel. The substitutions that impair NE- and PE-dependent activation result from changing of residues that are most likely to be good substrates based on the known primary amino acid specificities of the proteases to less preferred residues. Finally, heterologously expressed rat ENaC (Caldwell et al., 2005) and human ENaC (Harris et al., 2007) can be activated by NE which is consistent with the conservation of γV193 between the two species. Moreover, alignment of human, rat, mouse, and rabbit γ ENaC sequences show V182, V193, and A190 are conserved. These observations concur to implicate direct protease–ENaC interactions in channel activation.

Inferences about the nature of the protease–ENaC interaction can be drawn from the protease-activated current trajectories. From the analysis of the progress curves for current activation, the k_{obs} dependence on enzyme concentration suggests that activation requires at least two steps; an initial reversible step and a secondary rate-limiting activation step. If proteases interact directly with the channel, then the first step is C + E↔C•E, a rapid equilibrium from the association of channel (C) and enzyme (E). If the reaction is limited to one step where species C•E is the activated channel, the current trajectory would contain relaxation rate constants or k_{obs} according to k_{on}•[E] + koff, which represents a linear dependence of k_{obs} on enzyme concentration. Since the measured k_{obs} was not linear but hyperbolic, C•E is not the activated channel. At least one additional concentration-independent step is rate limiting, which may correspond to one or more possible physical states that represent the activated channel. One parsimonious interpretation is that the rate-limiting step includes hydrolysis. We found that the efficiency parameter k_{cat}/K_M for NE is on the order of the k_{cat}/K_M for the highest efficiencies of NE hydrolysis of its best extended synthetic substrates (i.e., substrates encompassing amino and carboxyl ends of the scissile bond; Koehl et al., 2003). It is noteworthy that the ratio of k_{cat}/K_M for the change of V residues to G residues for NE, and A residue to G residue for PE were also consistent with k_{cat}/K_M ratios for the same P1 residue changes in synthetic substrates (Zimmerman and Ashe, 1977; Nakajima et al., 1979; Koehl et al., 2003). In fact, the K_M determined for NE is remarkably similar to the dissociation constant for the NE α proteinase inhibitor complex (Mellet et al., 1998).

There are also examples of TH cleavage of its synthetic peptide substrates such as the protease-activated receptor 1 peptides (Vu et al., 1991) and natural substrates such as protein C (De Cristofaro and Landolfi, 1999) with similar k_{cat}/K_M as observed for TH activation of I_{Na} in the results presented. Hydrolysis is further suggested by the MALDI-TOF mass spectrometry performed on the synthetic peptide, which confirmed that NE cleavage is located between V193 and M194 while PE cleavage is located between A190 and S191 in the γ subunit. Thrombin cleaved the T^{176}-S^{198} peptide when substituted with a thrombin consensus sequence as well as the in vitro–translated γ_{Th} ENaC subunit. Harris et al. (2007) have recently shown that NE can cleave the γ subunit when expressed in *Xenopus* oocytes.

The results of the kinetic analysis of the progress curves, peptide T^{176}-S^{198} digestions, and thrombin cleavage of γ_{Th} are consistent with hydrolysis-dependent channel activation but cannot exclude other possibilities. These include the possibility that the k_{cat} represents a rate-limiting intramolecular rearrangement occurring long after cleavage, perhaps related to the Na^+ self inhibition of the channel (Chraibi and Horisberger, 2002; Sheng et al., 2006) or removal of an inhibitory domain (Carattino et al., 2006; Bruns et al., 2007). Secondarily, protease binding to the channel is sufficient to create a rate-limiting step including binding-dependent prevention of tonic inhibition by an ENaC cofactor or binding-induced conformational changes that directly activate the channel. Experiments so far do not rule out the latter two, as it can be imagined that a binding-induced conformational change is sufficient to activate the channel; and an accompanying hydrolysis ensues but has no significance. That the results are consistent with hydrolysis is in line with other studies showing that ENaC expressed at the apical membrane can be cleaved by furin and this cleavage correlates with channel activity (Hughey et al., 2004b). Also, the extent of channel cleavage correlates inversely with the trypsin activation of current (Knight et al., 2006), suggesting that once cleaved by endogenous proteases, channels may no longer be activated by trypsin. There is however evidence suggesting that the aprotinin-sensitive, trypsin-activated current may not be related to the cleavage patterns observed. In alveolar epithelial cells expressing CAP1, an ENaC-mediated I_{Na} sensitive to aprotinin inhibition and trypsin reversal, a presumably cleaved fragment of the α subunit is expressed at the apical membrane (Planes et al., 2005). The abundance of this fragment was not affected by aprotinin. In A6 cells, aprotinin inhibition of I_{Na} did not change the relative abundance of the low molecular weight species of the α subunit, nor have any effect on the γ subunit (Adebamiro et al., 2005). Furthermore, it was recently shown that mouse CAP1 lacking a catalytic triad retained the ability to activate ENaC (Andreasen et al., 2006). Therefore, furin-independent catalytic and noncatalytic mechanisms remain likely possibilities in channel activation by proteases. Further experiments are needed to determine if the catalytic activity of the exogenous proteases is required or if binding is sufficient to lead to activation. If cleavage is a prerequisite for channel activation then one must demonstrate the cleaved fragments form active channels.

The results of this study have important implications for ENaC regulation by proteases. First, extracellular proteases can produce a graded Na^+ transport response over a short time scale. If activation is irreversible, then eventual activation of all channels should occur over extended periods. From the results, the plateau current elicited by NE, PE, and TH correlates with the rate of activation. The plateau values may result from a steady state between protease activation and channel inactivation. The turnover time for ENaC in the membrane varies considerably from biochemical measurements from a few minutes to several hours (Weisz et al., 2000; Alvarez de la Rosa et al., 2002; Hanwell et al., 2002). However, functional experiments in FRT cells suggest a turnover time for channels of ∼30 min (Snyder, 2000).

If the NE- and PE-activated channels in FRT cells in the present study have the same turnover time as channels in the baseline condition, then the steady-state current would depend on the rate of protease activation. By changing the rate of protease activation, up- and down-regulation of epithelial Na^+ transport can be achieved within a 30-min window. Alternatively, the extent of protease activation could be altered by reducing the deactivation of channels. Recent studies showed that protease activation of ENaC could be up-regulated by maneuvers known to impair channel internalization (Knight et al., 2006). A graded response may also result from an equilibrium association of channel and protease. This association would not be a Michealis-Menten complex but involve further complex rearrangements typical of tight binding proteinase–inhibitor complexes (Beynon and Bond, 1996). Second, predictably from the turnover times and k_{cat}, the concentration of protease needed to achieve channel activation can be quite low. This is clearly evident for the thrombin case where the half maximal concentration was ~15 nM. Consequently, inadvertent activation of ENaC in inflammatory states such as chronic obstructive pulmonary disease and cystic fibrosis could result from the increased proteases in the local environment (Stockley, 2000) and may be involved in exacerbation of obstructive airways disease. Third, it is noteworthy that only one region was found to be critical for NE-mediated activation. However, multiple furin cleavage sequences were found to be important in the α subunit and in the γ subunit (Hughey et al., 2004a; Sheng et al., 2006). Because of a lack of strict adherence of NE to valines at the P1 position in its substrate, the valine substitution approach may miss other important P1 positions for NE interaction. Therefore, under aprotinin-treated conditions, it cannot be ruled out that NE/PE interacts also at the α subunit. On the other hand, with TH there is reduced likelihood of such an interaction and the results would suggest that interaction at one site in the γ subunit was sufficient for activation. Perhaps, under the aprotinin-treated conditions the α subunits are already cleaved and do not require further cleavage for channel activation. It is emphasized that these conclusions arise in the context of an aprotinin-inhibited state that does not represent the nascent channel state. As a result, ENaC may be acted upon by intra- and extracellular proteases, possibly in a serial fashion, and the segment investigated in this study may represent the site of action of an endogenous protease at the apical membrane.

We thank Drs. John P. Johnson and Neil Bradbury for many valuable suggestions. FRT cells were a gift from Dr. Peter Snyder (University of Iowa College of Medicine, Iowa City, IA). We thank Dr. Glucksman and Dr. Yuanda for help with MALDI-TOF analysis.

Studies were supported by National Institutes of Health grant RO1 DK-61639, National Research Service Award F31DK015311, National Center for Research Resources S10RR19325, Health Resources and Services Administration grant C76 HF03610-01-00, United Negro College Fund-Merck graduate research fellowship, and Novartis.

Lawrence G. Palmer served as editor.

Submitted: 12 March 2007
Accepted: 24 October 2007

REFERENCES

Adebamiro, A., Y. Cheng, J.P. Johnson, and R.J. Bridges. 2005. Endogenous protease activation of ENaC: effect of serine protease inhibition on ENaC single channel properties. *J. Gen. Physiol.* 126:339–352.

Alvarez de la Rosa, D., H. Li, and C.M. Canessa. 2002. Effects of aldosterone on biosynthesis, traffic, and functional expression of epithelial sodium channels in A6 cells. *J. Gen. Physiol.* 119:427–442.

Andreasen, D., G. Vuagniaux, N. Fowler-Jaeger, E. Hummler, and B.C. Rossier. 2006. Activation of epithelial sodium channels by mouse channel activating proteases (mCAP) expressed in *Xenopus* oocytes requires catalytic activity of mCAP3 and mCAP2 but not mCAP1. *J. Am. Soc. Nephrol.* 17:968–976.

Auerswald, E.A., D. Horlein, G. Reinhardt, W. Schroder, and E. Schnabel. 1988. Expression, isolation and characterization of recombinant [Arg15,Glu52]aprotinin. *Biol. Chem. Hoppe Seyler.* 369(Suppl.):27–35.

Baugh, R.J., and J. Travis. 1976. Human leukocyte granule elastase: rapid isolation and characterization. *Biochemistry.* 15:836–841.

Bengrine, A., J. Li, L.L. Hamm, and M.S. Awayda. 2007. Indirect activation of the epithelial Na^+ channel by trypsin. *J. Biol. Chem.* 282:26884–26896.

Beynon, R.J., and J.S. Bond. 1996. Proteolytic Enzymes. Vol. 1. Oxford University Press, New York. 83–102.

Bridges, R.J., B.B. Newton, J.M. Pilewski, D.C. Devor, C.T. Poll, and R.L. Hall. 2001. Na^+ transport in normal and CF human bronchial epithelial cells is inhibited by BAY 39-9437. *Am. J. Physiol. Lung Cell. Mol. Physiol.* 281:L16–L23.

Bruns, J.B., M.D. Carattino, S. Sheng, A.B. Maarouf, O.A. Weisz, J.M. Pilewski, R.P. Hughey, and T.R. Kleyman. 2007. Epithelial Na^+ channels are fully activated by furin- and prostasin-dependent release of an inhibitory peptide from the γ-subunit. *J. Biol. Chem.* 282:6153–6160.

Caldwell, R.A., R.C. Boucher, and M.J. Stutts. 2004. Serine protease activation of near-silent epithelial Na^+ channels. *Am. J. Physiol. Cell Physiol.* 286:C190–C194.

Caldwell, R.A., R.C. Boucher, and M.J. Stutts. 2005. Neutrophil elastase activates near-silent epithelial Na^+ channels and increases airway epithelial Na^+ transport. *Am. J. Physiol. Lung Cell. Mol. Physiol.* 288:L813–L819.

Canessa, C.M., L. Schild, G. Buell, B. Thorens, I. Gautschi, J.D. Horisberger, and B.C. Rossier. 1994. Amiloride-sensitive epithelial Na^+ channel is made of three homologous subunits. *Nature.* 367:463–467.

Carattino, M.D., S. Sheng, J.B. Bruns, J.M. Pilewski, R.P. Hughey, and T.R. Kleyman. 2006. The epithelial Na^+ channel is inhibited by a peptide derived from proteolytic processing of its α subunit. *J. Biol. Chem.* 281:18901–18907.

Chraibi, A., and J.D. Horisberger. 2002. Na self inhibition of human epithelial Na channel: temperature dependence and effect of extracellular proteases. *J. Gen. Physiol.* 120:133–145.

Chraibi, A., V. Vallet, D. Firsov, S.K. Hess, and J.D. Horisberger. 1998. Protease modulation of the activity of the epithelial sodium channel expressed in *Xenopus* oocytes. *J. Gen. Physiol.* 111:127–138.

De Cristofaro, R., and R. Landolfi. 1999. Allosteric modulation of BPTI interaction with human α- and ζ-thrombin. *Eur. J. Biochem.* 260:97–102.

Donaldson, S.H., A. Hirsh, D.C. Li, G. Holloway, J. Chao, R.C. Boucher, and S.E. Gabriel. 2002. Regulation of the epithelial sodium channel by serine proteases in human airways. *J. Biol. Chem.* 277:8338–8345.

Ergonul, Z., G. Frindt, and L.G. Palmer. 2006. Regulation of maturation and processing of ENaC subunits in the rat kidney. *Am. J. Physiol. Renal Physiol.* 291:F683–F693.

Firsov, D., L. Schild, I. Gautschi, A.M. Merillat, E. Schneeberger, and B.C. Rossier. 1996. Cell surface expression of the epithelial Na channel and a mutant causing Liddle syndrome: a quantitative approach. *Proc. Natl. Acad. Sci. USA.* 93:15370–15375.

Garty, H., and L.G. Palmer. 1997. Epithelial sodium channels: function, structure, and regulation. *Physiol. Rev.* 77:359–396.

Hanwell, D., T. Ishikawa, R. Saleki, and D. Rotin. 2002. Trafficking and cell surface stability of the epithelial Na^+ channel expressed in epithelial Madin-Darby canine kidney cells. *J. Biol. Chem.* 277:9772–9779.

Harris, M., D. Firsov, G. Vuagniaux, M.J. Stutts, and B.C. Rossier. 2007. A novel neutrophil elastase inhibitor prevents elastase activation and surface cleavage of the epithelial sodium channel expressed in *Xenopus laevis* oocytes. *J. Biol. Chem.* 282:58–64.

Hartley, B.S., and D.M. Shotton. 1971. The Enzymes. Vol. 3. Academic Press Inc., Orlando, FL. 323 pp.

Hughey, R.P., J.B. Bruns, C.L. Kinlough, K.L. Harkleroad, Q. Tong, M.D. Carattino, J.P. Johnson, J.D. Stockand, and T.R. Kleyman. 2004a. Epithelial sodium channels are activated by furin-dependent proteolysis. *J. Biol. Chem.* 279:18111–18114.

Hughey, R.P., J.B. Bruns, C.L. Kinlough, and T.R. Kleyman. 2004b. Distinct pools of epithelial sodium channels are expressed at the plasma membrane. *J. Biol. Chem.* 279:48491–48494.

Jenny, R.J., K.G. Mann, and R.L. Lundblad. 2003. A critical review of the methods for cleavage of fusion proteins with thrombin and factor Xa. *Protein Expr. Purif.* 31:1–11.

Kemmner, W., and K. Zaar. 1991. Rapid aggregation and tight junction formation in single cell suspensions of tumor cells after very low dose trypsin treatment. *FEBS Lett.* 281:43–46.

Knight, K.K., D.R. Olson, R. Zhou, and P.M. Snyder. 2006. Liddle's syndrome mutations increase Na^+ transport through dual effects on epithelial Na^+ channel surface expression and proteolytic cleavage. *Proc. Natl. Acad. Sci. USA.* 103:2805–2808.

Koehl, C., C.G. Knight, and J.G. Bieth. 2003. Compared action of neutrophil proteinase 3 and elastase on model substrates. Favorable effect of S'-P' interactions on proteinase 3 catalysts. *J. Biol. Chem.* 278:12609–12612.

Liu, L., K.S. Hering-Smith, F.R. Schiro, and L.L. Hamm. 2002. Serine protease activity in m-1 cortical collecting duct cells. *Hypertension.* 39:860–864.

Lynch, R.D., L.J. Tkachuk-Ross, J.M. McCormack, K.M. McCarthy, R.A. Rogers, and E.E. Schneeberger. 1995. Basolateral but not apical application of protease results in a rapid rise of transepithelial electrical resistance and formation of aberrant tight junction strands in MDCK cells. *Eur. J. Cell Biol.* 66:257–267.

Margolius, H.S., and J. Chao. 1980. Amiloride inhibits mammalian renal kallikrein and a kallikrein-like enzyme from toad bladder and skin. *J. Clin. Invest.* 65:1343–1350.

Masilamani, S., G.H. Kim, C. Mitchell, J.B. Wade, and M.A. Knepper. 1999. Aldosterone-mediated regulation of ENaC α, β, and γ subunit proteins in rat kidney. *J. Clin. Invest.* 104:R19–R23.

McDonald, F.J., P.M. Snyder, P.B. McCray Jr., and M.J. Welsh. 1994. Cloning, expression, and tissue distribution of a human amiloride-sensitive Na^+ channel. *Am. J. Physiol.* 266:L728–L734.

Mellet, P., C. Boudier, Y. Mely, and J.G. Bieth. 1998. Stopped flow fluorescence energy transfer measurement of the rate constants describing the reversible formation and the irreversible rearrangement of the elastase-α1-proteinase inhibitor complex. *J. Biol. Chem.* 273:9119–9123.

Meyer, H.W., C. Freytag, T. Freytag, and W. Richter. 1988. Effect of proteases and other treatments on the proliferative assembly of tight junction strands in the rat prostate tissue. *Exp. Pathol.* 34:237–244.

Myerburg, M.M., M.B. Butterworth, E.E. McKenna, K.W. Peters, R.A. Frizzell, T.R. Kleyman, and J.M. Pilewski. 2006. Airway surface liquid volume regulates ENaC by altering the serine protease-protease inhibitor balance: a mechanism for sodium hyperabsorption in cystic fibrosis. *J. Biol. Chem.* 281:27942–27949.

Nakajima, K., J.C. Powers, B.M. Ashe, and M. Zimmerman. 1979. Mapping the extended substrate binding site of cathepsin G and human leukocyte elastase. Studies with peptide substrates related to the alpha 1-protease inhibitor reactive site. *J. Biol. Chem.* 254:4027–4032.

Nakhoul, N.L., K.S. Hering-Smith, C.T. Gambala, and L.L. Hamm. 1998. Regulation of sodium transport in M-1 cells. *Am. J. Physiol.* 275:F998–F1007.

Narikiyo, T., K. Kitamura, M. Adachi, T. Miyoshi, K. Iwashita, N. Shiraishi, H. Nonoguchi, L.M. Chen, K.X. Chai, J. Chao, and K. Tomita. 2002. Regulation of prostasin by aldosterone in the kidney. *J. Clin. Invest.* 109:401–408.

Ohlsson, K., and A.S. Olsson. 1976. Purification and partial characterization of human pancreatic elastase. *Hoppe Seylers Z. Physiol. Chem.* 357:1153–1161.

Orce, G.G., G.A. Castillo, and H.S. Margolius. 1980. Inhibition of short-circuit current in toad urinary bladder by inhibitors of glandular kallikrein. *Am. J. Physiol.* 239:F459–F465.

Pintigny, D., and J. Dachary-Prigent. 1992. Aprotinin can inhibit the proteolytic activity of thrombin. A fluorescence and an enzymatic study. *Eur. J. Biochem.* 207:89–95.

Planes, C., C. Leyvraz, T. Uchida, M.A. Angelova, G. Vuagniaux, E. Hummler, M.A. Matthay, C. Clerici, and B.C. Rossier. 2005. In vitro and in vivo regulation of transepithelial lung alveolar sodium transport by serine proteases. *Am. J. Physiol. Lung Cell. Mol. Physiol.* 288:L1099–L1109.

Poirot, O., M. Vukicevic, A. Boesch, and S. Kellenberger. 2004. Selective regulation of acid-sensing ion channel 1 by serine proteases. *J. Biol. Chem.* 279:38448–38457.

Scott, C.F., H.R. Wenzel, H.R. Tschesche, and R.W. Colman. 1987. Kinetics of inhibition of human plasma kallikrein by a site-specific modified inhibitor Arg15-aprotinin: evaluation using a microplate system and comparison with other proteases. *Blood.* 69:1431–1436.

Sheng, S., M.D. Carattino, J.B. Bruns, R.P. Hughey, and T.R. Kleyman. 2006. Furin cleavage activates the epithelial Na^+ channels by relieving Na+ self-inhibition. *Am. J. Physiol. Renal Physiol.* 290:F1488–F1496.

Sheppard, D.N., M.R. Carson, L.S. Ostedgaard, G.M. Denning, and M.J. Welsh. 1994. Expression of cystic fibrosis transmembrane conductance regulator in a model epithelium. *Am. J. Physiol.* 266: L405–L413.

Snyder, P.M. 2000. Liddle's syndrome mutations disrupt cAMP-mediated translocation of the epithelial Na^+ channel to the cell surface. *J. Clin. Invest.* 105:45–53.

Snyder, P.M., D.R. Olson, R. Kabra, R. Zhou, and J.C. Steines. 2004. cAMP and serum and glucocorticoid-inducible kinase (SGK) regulate the epithelial Na^+ channel through convergent phosphorylation of Nedd4-2. *J. Biol. Chem.* 279:45753–45758.

Stockley, R.A. 2000. New approaches to the management of COPD. *Chest.* 117:58S–62S.

Takagi, T., and R.F. Doolittle. 1974. Amino acid sequence studies on factor XIII and the peptide released during its activation by thrombin. *Biochemistry.* 13:750–756.

Tavernarakis, N., and M. Driscoll. 1997. Molecular modeling of mechanotransduction in the nematode *Caenorhabditis elegans. Annu. Rev. Physiol.* 59:659–689.

Travis, J., P.J. Giles, L. Porcelli, C.F. Reilly, R. Baugh, and J. Powers. 1979. Human leucocyte elastase and cathepsin G: structural and functional characteristics. *Ciba Found. Symp.* 75:51–68.

Vallet, V., A. Chraibi, H.P. Gaeggeler, J.D. Horisberger, and B.C. Rossier. 1997. An epithelial serine protease activates the amiloride-sensitive sodium channel. *Nature.* 389:607–610.

Vu, T.K., V.I. Wheaton, D.T. Hung, I. Charo, and S.R. Coughlin. 1991. Domains specifying thrombin-receptor interaction. *Nature.* 353:674–677.

Vuagniaux, G., V. Vallet, N.F. Jaeger, E. Hummler, and B.C. Rossier. 2002. Synergistic activation of ENaC by three membrane-bound channel-activating serine proteases (mCAP1, mCAP2, and mCAP3) and serum- and glucocorticoid-regulated kinase (Sgk1) in *Xenopus* oocytes. *J. Gen. Physiol.* 120:191–201.

Vukicevic, M., G. Weder, A. Boillat, A. Boesch, and S. Kellenberger. 2006. Trypsin cleaves acid-sensing ion channel 1a in a domain that is critical for channel gating. *J. Biol. Chem.* 281:714–722.

Weisz, O.A., J.M. Wang, R.S. Edinger, and J.P. Johnson. 2000. Non-coordinate regulation of endogenous epithelial sodium channel (ENaC) subunit expression at the apical membrane of A6 cells in response to various transporting conditions. *J. Biol. Chem.* 275:39886–39893.

Zimmerman, M., and B.M. Ashe. 1977. Substrate specificity of the elastase and the chymotrypsin-like enzyme of the human granulocyte. *Biochim. Biophys. Acta.* 480:241–245.